QATAR UNIVERSITY

COLLEGE OF ENGINEERING

FLEXURAL BEHAVIOR OF BASALT FIBER REINFORCED ONE-WAY CONCRETE SLABS REINFORCED WITH FIBER REINFORCED POLYMER BARS

BY

YOUSEF ADNAN OMER RIHAN

A Thesis Submitted to

the Faculty of The College of

Engineering

In Partial Fulfillment

of the Requirements

for the Degree of

Master of Science in Civil Engineering

January 2018

COMMITTEE PAGE

The members of the Committee approve the Thesis of Yousef Adnan Omer Rihan defended on 13/12/2017.

Dr. Wael Alnahhal
Thesis Supervisor

Dr. Mohammed Alansari
Committee Member

Dr. Ahmed Alrifai
Committee Member

Dr. Alaa Alhawari
Committee Member

Approved:

Khalifa Al-Khalifa, Dean, College of Engineering

ABSTRACT

Rihan Yousef Adnan. Masters of Science in Civil Engineering.

January: 2018

Title: Flexural Behavior of Basalt Fiber Reinforced One-Way Concrete Slabs Reinforced with Fiber Reinforced Polymer Bars

Supervisor of Thesis: Dr. Wael Ibrahim Alnahhal

The State of Qatar suffers from a harsh environment in the form of high temperature that prevails almost all year round, in addition to severe humidity and coastal conditions. This exposure leads to the rapid deterioration and the reduction of the life span of reinforced concrete (RC) infrastructure. The full functionality and safe use of the infrastructure in such an environment can only be maintained by using holistic approaches including the use of advanced materials for new construction. This study will, therefore, investigate the feasibility of using advanced composites, especially fiber reinforced polymer (FRP) materials as viable alternatives to traditional construction materials.

The purpose of this study is to investigate the flexural performance, serviceability and ultimate capacity of basalt fiber reinforced concrete (BFRC) one-way concrete slabs reinforced with FRP bars experimentally and analytically. A total of 12 BFRC one-way concrete slab specimens were flexural tested until failure. The parameters investigated included the type of reinforcement (Basalt FRP bars and Glass FRP bars), reinforcement ratio ($1.4\rho_{fb}$ and $2.8\rho_{fb}$), and the basalt macro-fiber (BMF) volume fraction (0%, 0.5%, 1% and 2%). The deflection, tensile bars strain and compressive concrete strain at mid-span of the slab were measured and recorded. The testing results of the specimens were compared to the control specimens. Test results showed that cracking moment, ultimate

moment, mid span deflection and ductility index were improved with the addition of both the BMF and the main reinforcement ratio. Deflection and capacity were calculated analytically using different codes and guidelines, compared to the tested results the results were acceptable. Test results clearly showed that both BFRP bars and BMF can be used as an alternative material in concrete structures at the State of Qatar.

ACKNOWLEDGMENT

I would like to give my full thankful to my parents who never stopped supporting me through their prayers, ongoing advice, and providing me the appropriate atmosphere for studying and succeeding in life. Also, I am sincerely grateful to my thesis supervisor Dr. Wael Alnahhal for his support, advice and consulting. His way of thinking, decision-making and managing significantly helped me to complete this research. I would also like to show my appreciation to Qatar University who gave me the chance to complete my master program and their financial support to finalize my research. Furthermore, I will never forget the help I got from Eng. Mohammed Elbardaweel and Eng. Abdulaziz from Qatar University during the experimental work of my research.

TABLE OF CONTENTS

LIST OF FIGURES

LIST OF TABLES

NOMENCLATURE

AFRP	Aramid Fiber Reinforced Polymer
BFRP	Basalt Fiber Reinforced Polymer
BMF	Basalt Macro-Fiber
CFRP	Carbon Fiber Reinforced Polymer
FRC	Fiber Reinforced Concrete
FRP	Fiber Reinforced Polymer
GFRP	Glass Fiber Reinforced Polymer
LVDT	Liner Variable Differential Transducer
RC	Reinforced Concrete
SFRC	Steel Fiber Reinforced Concrete
SMF	Steel Macro-Fibers
SRC	Steel Reinforced Concrete

SYMBOLS

A_f	The cross-sectional area of FRP reinforcing bars
A_{fr}	The required area of FRP reinforcing bars
A_{cf}	The area of basalt macro-fibers in compressive zone
A_{tf}	The area of basalt macro-fibers in tensile zone
a	The distance between the support and the nearest point load
b	The beam sample width
C_E	The environmental reduction factor
c	The distance from extreme compression fiber to the neutral axis
d	The beam sample effective depth
d_{fi}	The fiber diameter
E_c	The modulus of elasticity of concrete
E_e	The elastic absorbed energy
E_f	The design or guaranteed modulus of elasticity of FRP
E_{fi}	The fiber modulus of elasticity
E_s	The steel modulus of elasticity
E_t	The total absorbed energy

e	The distance from extreme compression fiber to top of tensile stress block of fibrous concrete
F_{be}	The bond efficiency of the fiber
f'_c	The specified compressive strength of concrete
f_f	The tension stress of FRP reinforcement bars
f_{fu}	The design tensile strength of FRP
f^*_{fu}	The guaranteed tensile strength of an FRP bar
f_r	The rupture strength of concrete
h	The beam sample actual depth
I_{cr}	The cracking moment of inertia
I_e	The effective moment of inertia
I_g	The gross moment of inertia
I_m	The average moment of inertia
k	The ratio of the depth of the neutral axis to the reinforcement depth
L	The beam span length
l_{fi}	The length of basalt macro-fibers
M_a	The service moment at the critical cross-section of the beam
M_{cr}	The cracking moment

$M_{cr_{exp.}}$ The Experimental Cracking Moment

$M_{cr_{theo.}}$ The Theoretical Cracking Moment

M_n The theoretical ultimate moment

M_u The experimental ultimate moment

n_f The ratio of the modulus of elasticity of FRP bars to the modulus of elasticity of concrete

P The total load applied by the universal test machine

P_{cr} The experimental cracking load

P_u The experimental ultimate load

T_b The tension force of FRP reinforcing bars

T_{fi} The tension force of fibrous concrete

V_f The basalt macro-fiber volume fraction

y_t The distance from centroidal axis of gross section, neglecting reinforcement, to tension face

α_b The bond dependent coefficient

β_1 A factor relating depth of equivalent rectangular compressive stress block to neutral axis depth

β_d A reduction coefficient

δ_{cr} The deflection of the cracking point

δ_{crd} The deflection of the cracked section

δ_f The deflection at failure

δ_g The deflection of the gross section

δ_{max} The maximum deflection

ε_{cu} The maximum usable strain at extreme concrete compression fiber

ε_{fi} The fiber tensile strain

η_0 The orientation factor before cracking

η'_0 The orientation factor after cracking

η_l The length efficiency factor

$\rho_{1.4}$ The balance reinforced ratio used in this research

$\rho_{2.8}$ The over-reinforced ratio used in this research

ρ_f The actual reinforcement ratio

ρ_{fb} The balance reinforced ratio

σ_{fi} The fiber stress

σ_T The tensile stress in fibrous concrete

μ_E The ductility index

CHAPTER 1: INTRODUCTION

Rehabilitation of deteriorated Civil Engineering structure has been a major issue in the last decades. The deterioration of these structures might be due to aging, poor maintenance, poor maintenance and corrosion due to environmental conditions. Especially in the Gulf region, the region is known for its harsh environment and severe weather conditions. In Qatar, the temperature is high and the humidity present is huge in addition to high chloride content in the soil, due to the harsh environmental conditions, the RC structures show a large reinforcement corrosion, concrete deterioration, and cracks. With the developments in materials science, the advanced composites, especially FRP materials are becoming viable alternatives to the traditional construction materials. Having superior durability against corrosion, versatility for easy in-situ applications and enhanced weight-to-strength ratios compared to their counterpart conventional materials, FRPs are promising to be the future of construction materials. Although there is no particular limit for their shape, FRPs are mostly used for reinforcing the structural members instead of steel reinforcement in Civil Engineering applications. Design guidelines and national standards for FRP reinforced structures have been developed grace to the numerous studies conducted by many researchers. Carbon, Glass and Aramid FRP are the commonly available FRPs used in the industry. Glass FRP (GFRP) is normally the one currently used in Civil Engineering applications. However, GFRP composites are affected by stress corrosion and creep failure. More recently, FRP composites made of basalt FRP (BFRP) have been introduced as an alternative to traditional steel reinforcement at a price comparable to glass fibers of about $2.5–5.0 per kg, which is significantly lower than carbon fibers.

Basalt fiber is a good alternative to steel reinforcement, due to better chemical resistance. On the other hand, some reports showed that if basalt immersed in alkaline solutions degradation is found for tensile modulus, strength, and elongation at breakage. That Degradation in tensile modulus is due to the variation in the producing processing and mineral components of basalt fiber. Intensive experimental testing is required to determine the mechanical and chemical properties for the BFRP. FRP reinforced bars has a low modulus of elasticity compared with steel bars, it is about 4 times smaller than the modulus of elasticity of steel, and that will lead to a higher deformation of one-way slabs reinforced with BFRP and larger cracks widths when compared with one-way slabs reinforced with normal steel bars. An experimental result is needed to check the deflection and crack width for the serviceability limit state.

BFRP bars are week in a brittle manner compared to steel bars. In addition to that it is known that high-strength concrete is brittle, and to overcome the brittle failure fiber reinforced concrete (FRC) is used as a good alternative solution and to increase the ductility of high-strength RC. To increase the ductility of concrete steel macro-fibers (SMF) is used, due to the large compressive strains showed at failure. There are limited research studies on the structural performance of concrete structures reinforced with FRP, moreover, the use of chopped basalt fiber and the BFRP reinforced bars. There is a new way to reduce the crack width and to overcome the deficiencies of FRC with naked basalt fiber, this new product was developed by ReforceTech AS, Norway the product carries the name (MiniBars). MiniBar is a non-corrosive structural macro-fiber made from BFRP. This material allows mixing of concrete with sufficiently large volumes of fiber without impairing the walkability. The density of BMF is almost equal the density of concrete and

that will give the BMF an advantage over other fiber options during the mixing of concrete. Numerous applied applications have been successfully demonstrated that BMF is suitable for FRC applications. Mixing the BMF with concrete at a dosage ranging from 0.3% to 4% by volume will not affect the workability and it was practical. In addition to that BMF acts as the proactive reinforcement that provides the immediate tensile load carrying capacity when micro-cracks develop in concrete. BMF has a tensile strength of 1080 MPa and a modulus of elasticity of 44 GPa.

This study is investigating the feasibility of using different volume fractions of BMF in FRC one-way concrete slabs reinforced with basalt or glass FRP bars. This is one of the pioneer research efforts, which examines the effect of using BMF on the flexural behavior and ultimate capacity of FRC one-way concrete slabs with two different main reinforcement ratios experimentally and analytically. As well, the second interconnected part of this study was calculating the deflection of the tested one-way concrete slabs analytically by comparing the experimental results with the existing current code-based equations.

1.1 RESEARCH SIGNIFICANCE

The environment in Qatar is harsh not only for inhabitants but for the high rising structures lining its skyline as well. Most importantly, RC structures which are the primary construction material are vulnerable to corrosion, cracking and premature deterioration. Therefore, new materials must be developed to overcome these challenges. With recent advances in the development of high-performance composite materials and the escalation of the cost of conventional materials, the time may now be right for the development of new alternatives construction materials such as BFRP composites in combination with

concrete is a possible solution to enhance the structural performance of concrete structures. (BFRP) poses new challenges due to its low modulus of elasticity, also the high deflections and large crack widths. Moreover, the brittleness of FRP reinforced structures limiting their usage in seismically active regions where the structure ductility is vital to resist oscillating loads. Furthermore, concrete itself is a brittle material and high-strength concrete is even more brittle. SMF that were tested in concrete has shown increases in the ductility of the concrete due to the large compressive strains exhibited at failure. However, it has a main disadvantage which is corrosion especially in the harsh environment that characterizes the Gulf. In this study, BMF, trademarked as MiniBar is introduced as an alternative building material in order to overcome the serviceability and ductility barriers.

The test results of this project will shed light on the feasibility of using MiniBar fibers to enhance the flexural performance of concrete one-way slabs reinforced with BFRP bars. It will also provide a better understanding of failure mechanisms of MRC one-way slabs reinforced with BFRP bars and ultimate capacity. The provided results of this project will have a significant influence on the use of FRC in the gulf area especially in Qatar where the harsh environment is dominating. In this aspect, the application of this anti-corrosive basalt fiber in the structural field will solve the disadvantage of steel reinforcement/fibers corrosion. Using basalt fibers in RC structures will lead to more sustainable structure by having little to no maintenance cost during their service life and thereby reduce their overall life-cycle cost. To the best of the authors' knowledge, this research project on the flexural behavior of FRC one-way slabs reinforced with BFRP bars is the first conducted research project in the GCC region.

RC structures are the most common type of buildings in Qatar and GCC countries. Concrete is very sensitive to harsh environment features of GCC countries like humidity and extremely high temperatures. Such a weather makes RC structures significantly affected by the corrosion of steel reinforcing bars, cracking and premature deterioration. So that it is the time to come up with new construction materials to be ideal alternatives of traditional materials with more strength and better resistance to harsh environmental effects. BFRP is a composite material developed to be one of these alternatives. BFRP poses new challenges due to its low modulus of elasticity, also the high deflections and large crack widths. Moreover, the brittleness of FRP reinforced structures limiting their usage in seismically active regions where the structure ductility is vital to resist oscillating loads. Furthermore, concrete itself is a brittle material and high-strength concrete is even more brittle. SMF that were tested in concrete has shown increases in the ductility of the concrete due to the large compressive strains exhibited at failure. However, it has a main disadvantage which is corrosion especially in the harsh environment that characterizes the Gulf. In this study, BMF, trademarked as MiniBar is introduced as an alternative building material in order to overcome the serviceability and ductility barriers.

The study will shed light on the feasibility of using BMF to enhance the flexural performance of concrete one-way slabs reinforced with FRP bars. It will also provide a better understanding of the failure mechanisms of BFRC one-way slabs reinforced with FRP bars and the ultimate capacity. The outcome of this research study will have a significant influence on the use of FRC in the gulf area especially at Qatar where the harsh environment is dominating. In this aspect, the application of this anti-corrosive basalt fiber in the structural field will solve the disadvantage of steel reinforcement/fibers corrosion.

Using basalt fibers in RC structures will lead to more sustainable structure by having little to no maintenance cost during their service life and thereby reduce their overall life-cycle cost. To the best of the authors' knowledge, this research project on the flexural behavior of FRC one-way slabs reinforced with BFRP bars is the first conducted research project in the GCC region.

1.2 RESEARCH OBJECTIVES

This study is designed to achieve the following main objectives:

1- Investigate the effects of adding BMF in different volume fractions on the flexural behavior of BFRC one-way concrete slabs reinforced with FRP bars.

2- Investigate experimentally the serviceability performance of the basalt FRC one-way concrete slabs reinforced with BFRP bars in terms of deflection and crack patterns.

3- Study and compute the load-carrying capacity experimentally and analytically of BFRC one-way concrete slabs reinforced with FRP bars. The scope of the study includes ductility of the one-way concrete slabs, failure mechanisms, and modes of failures.

4- Investigate experimentally the effect of the type of reinforcement and the reinforcement ration on the flexural behavior of BFRC one-way concrete slabs reinforced with FRP bars.

5- Provide analytical equations to predict the deflection and moment capacity of FRC one-way concrete slabs reinforced with FRP bars.

CHAPTER 2: BACKGROUND AND LITERATURE REVIEW

2.1 BASALT FIBER REINFORCED POLYMER REINFORCING BARS

FRP materials were accepted widely as reinforcing materials for concrete buildings due to their positive properties such as high strength to weight ratio, non-corrosive and non-magnetic materials. There have been a large number of studies to develop national standards and guidelines for FRP reinforced concrete structures (ACI Committee 440, 2006; ISIS Canada 2007; CSA, 2012; Japan Society of Civil Engineers, 1997). FRP reinforcing bars are made from different raw materials and get their names and properties from the main raw material that they are made of. The most common FRP reinforcing bars are Glass FRP (GFRP), Carbon FRP (CFRP) and Aramid FRP (AFRP). The most commonly used FRP materials are GFRP due to their affordable prices (Benmokrane, 2002). Recently, Basalt FRP (BFRP) reinforcing bars were available at affordable prices of about $2.5 to $5.0 per kg, which is cheaper than CFRP bars (Kameny, 2010). BFRP bars are an environmentally friendly material because basalt is produced through volcanic melted rocks without adding additives which makes it cheaper to produce than GFRP bars (Yilmaz, 1996; Wei, 2010). BFRP bars are attractive materials for researchers due to their tensile strength that is higher than E-glass, failure strain which is higher than CFRP bars and high thermal stability, BFRP bars' strength does not alter under high temperature and pressure (Benmokrane, 2002; Kameny, 2010; Fahmy, 2009; Erlendsson, 2012; Yilmaz, 1996; Sim, 2005; Berozashvili, 2001). BFRP bars have good resistance to ultra-violet exposure (Lee, 2002). On the other hand, BFRP bars lose a lot of their volume and strength when submerging them in alkali solution (Yilmaz, 1996; Sim, 2005; Li, 2012), but they are better than GFRP bars (Van De Velde, 2002). Other studies (Elrefai, 2013; Serbescu, 2014)

showed that BFRP bars have good resistance to alkaline solutions. The fluctuations in their properties are due to the different mineral components used by different manufacturers. BFRP bars have good resistance at a low concentration of acid solution but their acid resistance becomes weaker with high acid solution concentration (Xianqi, 2002; Mingchao, 2008). The more moisture absorbed by BFRP bars may cause severe degradation of BMF bars since moisture will plasticize the resin and may cause debonding between fiber and matrix (Mingchao, 2008; Xian, 2007). Beams reinforced by BFRP bars are exhibited to have higher deflection, more cracks and larger crack widths than beams reinforced by steel reinforcing bars because the modulus of elasticity of BFRP reinforcing bars is about 25% of the modulus of elasticity of steel reinforcing bars (Marek, 2013).

2.2 FIBER REINFORCED CONCRETE

BMF are inorganic fibers manufactured by melting processes in high temperatures form basaltic rocks. The possibility of producing fibers from basaltic rocks refers to the ability to crush them into very fine pieces. There are no additives used while producing basalt fibers, which makes them less costly than other fibers. Also, it is good to know that the BMF is greater in strain at failure than fibers made with carbon. In addition, they have better tensile strength than fibers made by E-glass (ACI Committee 318, 2011; ASTM C39/C39M-12a, 2012; High, 2015; Ma, 2011; Borhan, 2013; Berozashvili, 2001). There are different additives which could be added to the fresh concrete to enhance the pore structure of concrete matrix (Ayub, 2014). BMF is one of these concrete additives, it is commonly used in recent years to improve properties of hardened concrete and its durability (Khan, 2014; Memon, 2014; Ayub, 2013). They are better than SMF, which are adversely affected by humidity. The first time BMF was mentioned was in a report for the

Highway Innovations Deserving Exploratory Analysis (IDEA) Project 45 in 1998 (Ramakrishnan, 1998). BMF has a variety of good properties that positively affect concrete like enhancing its ductility index, so it is not affected by excessive temperature and chemical materials and also it isolates sound in good rates (Artemenko, 2003; Van De Velde, 2003). BMF Volume fraction differs due to the usage of concrete. To reduce the shrinkage cracking in pavement and slabs, the preferable volume fraction is less than 1%. To improve the concrete capability of absorbing high energy and improving resistance to delamination, fatigue, modulus of rupture and concrete fracture toughness it is better to add BMF between 1 and 2% of concrete volume fraction and more than 2% to obtain the concrete strain hardening behavior (Ayub, 2014; Mehta, 2006).

FRP bars were developed as an alternative to steel reinforcing bars. There are different types of FRP bars. Depending on the main raw material made of, FRP bar gains its name and properties. The most common FRP bars are Carbon FRP bars (CFRP), Glass FRP bars (GFRP) and Aramid FRP bars (AFRP).

BFRP bars have been currently commonly used around the world as an alternative to traditional steel reinforcing bars (Patnaik, 2004; Patnaik, 2009; Patnaik, 2010; Patnaik, 2011). It is manufactured from the same raw material of BMF with a common diameter varying between 13 and 20 mm. BFRP reinforcing bars have better chemical and mechanical performance than the traditional steel reinforcing bars. Another important aspect of the basalt fibers is fire resistance (Kim, 1999), so the structure will not easily affected easily by fire. BFRP bars have larger ultimate tensile strength than steel bars, which give more ultimate strength for concrete elements, but it is perfectly elastic material without any plastic performance.

The main problem of BFRP reinforced concrete is that both BFRP reinforcing bars and concrete are perfectly brittle materials and fail in a brittle manner. This makes the steel reinforced concrete (SRC) a preferable choice due to the ability of steel reinforcing bars to act in a plastic manner. The best solution to overcome the shortage in ductility of FRP reinforced concrete is enhancing concrete ductility by adding macro-fibers to the concrete mix (Yang, 2012). Concrete enhanced by macro-fibers is called fiber reinforced concrete (FRC). Macro-fibers are made from many raw materials and the most common and one is the SMF. ACI committee 544 is used for the design of FRC (ACI Committee 544, 1999). Research shows that adding SMF to concrete mix enhances its ductility and compressive strain at failure (Holschemacher, 2010; Mohammadi, 2009; Katzer, 2012). BMF have advantages on SMF as they are resistant to corrosion; this advantage is particularly important in GCC countries with their harsh weather. The other advantage is that they are higher in tensile strength than SMF (Adhikari, 2013). Polypropylene fiber concrete has higher crack width than FRC (Adhikari, 2013; Katzer, 2012). Another advantage of BMF is their density is close to the concrete density when compared with synthetic or steel fibers (Patnaik, 2012). The main setback of BMF is with increasing their volume fraction or length, the fresh concrete workability is decreasing (Iyer, 2015). However, using BMF with a volume fraction less or equal than 4% resulted in having a fresh concrete with good workability and acceptable slump (Patnaik, 2014). Oskarsson (2013) compared RC beams with 1% BMF volume fraction to RC beams without BMF. The ultimate strength, mid-span deflection at failure, bottom strain, and top strain were increased with the presence of BMF. Cracks in FRC started appearing at a load of 18 kN, meanwhile, in plain concrete, it appeared at 20 kN load. In plain concrete, beams lost all bearing capacity rapidly when

they reached their failure load, on the other hand, FRC beams lost around 40% of their bearing capacity when they reached their failure load initially and the rest was lost gradually. Wang (2005) compared concrete containing polypropylene fibers with plain concrete. At service load; crack widths were less in polypropylene fiber concrete compared to the crack widths of plain concrete and the ductility of polypropylene fiber concrete was larger by 40% (Wang, 2005). Also, the FRC is higher in strength than plain concrete (Reddy, 2015). A number of researchers compared FRC beams with different BMF volume fractions. They found that increasing volume fraction of BMF resulted in an increase in concrete cracking resistance, flexural strength and splitting behavior of concrete (Ayub, 2014; Jiang, 2014). Kara (2015) invented a numerical method for estimating the curvature, deflection and moment capacity of hybrid fiber reinforced polymer/steel fiber reinforced concrete beams and compared his results with experimental results from previous studies. His numerical technique gives an accurate prediction of moment capacity, curvature and deflection of hybrid fiber reinforced polymer/steel fiber reinforced concrete beams. The numerical results also indicate that beam ductility and stiffness are improved when steel reinforcement is added to FRP reinforced concrete beams (Kara, 2015). Sahoo (2015) found that cracks in FRC are more than cracks in plain concrete and it was increased with the increase of fiber volume fraction because fibers enhance the distribution of stresses along the concrete element.

2.3 FRP REINFORCED CONCRETE

FRP reinforcing bars are made from different materials and their properties vary due to the way they are manufactured despite them being from the same raw materials. These dissimilarities are because of differences in locations where the natural raw materials

come from, differences in manufacturing processes and variations of additives added and their concentrations. Consequently, codes and guidelines do not give perfectly accurate results for FRP reinforced concrete like SRC. A number of studies investigated the behavior of RC beams reinforced with FRP bars. Saikia (2007) investigated the flexural behavior beams reinforced with glass fiber reinforced polymer (GFRP) bars experimentally. The failure of GFRP reinforced concrete was due to the slippage of bars from the surrounding concrete. Saikia (2007) found that adding polypropylene fibers to the concrete gives secondary effect on post cracking of the concrete. He proposed an analytical model to predict the crack width and load deflection, which its results were very close to experimental results. Pecce (2000) tested concrete beams reinforced with two different reinforcement ratios of GFRP bars. Both samples failed due to flexural failure and the fracture of the GFRP bars. Habeeb (2008) studied GFRP reinforced concrete. The testing results revealed beams failed in four different failure modes: bar rapture, concrete crushing, and shear failure with concrete crushing and conventional ductile failure (Habeeb, 2008). Another study by Adam (2015) analyzed the flexural behavior of concrete beams, with different compressive strengths, reinforced with GFRP bars with different reinforcement ratios. Test results were compared to concrete beams reinforced with steel reinforcing bars. The test results revealed that crack widths and mid-span deflection were significantly decreased by increasing the reinforcement ratio. However, the ultimate load was increased when the reinforcement ratio was raised. El-Mogy (2010) compared GFRP, CFRP and steel reinforced concrete beams. Results showed higher deflection of FRP reinforced concrete than SRC (El-Mogy, 2010). High (2015) studied the effects of basalt reinforcing bars and BMF on concrete and compared results with ACI440.1R-06. Bonding between BFRP bars

and concrete was improved with the increase in the reinforcement ratios. This is one of the reasons to have a compression control design in beams reinforced with FRP bars as specified in ACI440.1R-06. Since BFRP bars have a low modulus of elasticity, the design of beams reinforced with FRP bars is mainly stiffness controlled. Other researchers showed that using of FRP reinforcing bars enhances concrete structures better than steel reinforcing bars (Mahroug, 2014; Lapko, 2015; Ashour, 2008; Banibayat, 2015; Barris, 2009). Ashour (2008) used ACI440.1R-06 equations and came up with predicted beams deflection until the excessive cracks level. However, because of losing bond between FRP bars and surrounding concrete ACI440.1R-06 equations for load capacity and deflection after excessive cracks level predictions were negatively affected (Ashour, 2008). Mahroug (2014) calculated deflection and moment capacity using ISIS-M03-07 and CSA S806-06 design guidelines. His results were closer to test results than ACI440.1R-06 predictions for BFRP reinforced concrete slabs (Mahroug, 2014). Kara (2013) found a significant difference between experimental results of FRP reinforced concrete beams and results calculated by the typical procedure of calculating the deflection of SRC beams (Kara, 2013). Ju (2016) compared experimental and analytical results of flexural capacity and moment deflection relationship for GFRP reinforced concrete beams and he got acceptable results (Ju, 2016).

CHAPTER 3: EXPERIMENTAL PROGRAM

3.1 MATERIALS CHARACTERIZATION

3.1.1 Basalt Macro-Fibers

BMF shown in Figure 1 is a corrosion resistant material since it is made from basalt stones and coated by a solution to be suitable for concrete. The average diameter of BMF used in this research is 0.66 mm with 42.5 mm length (Figures 2). With 1080 MPa tensile strength and 90 GPa modulus of elasticity, this material has the ability to give the concrete mix higher tensile strength and stiffness. Their mechanism is to be a proactive reinforcement that will provide an immediate tensile load which will carry the capacity when micro-cracks develop in concrete. Three different volume fraction of BMF will be studied in this research (0.5%, 1% and 2%). By studying 100×100×500 mm^3 FRC prisms to investigate their effect on concrete flexural performance and 175×500×2250 mm^3 FRP reinforced one-way concrete slabs to investigate their effects on flexure in presence of FRP reinforcing bars and compared with samples without BMF. The main properties of the BMF used are shown in Table 1 (ReforceTech, 2015).

Figure 1. Basalt Macro-Fibers

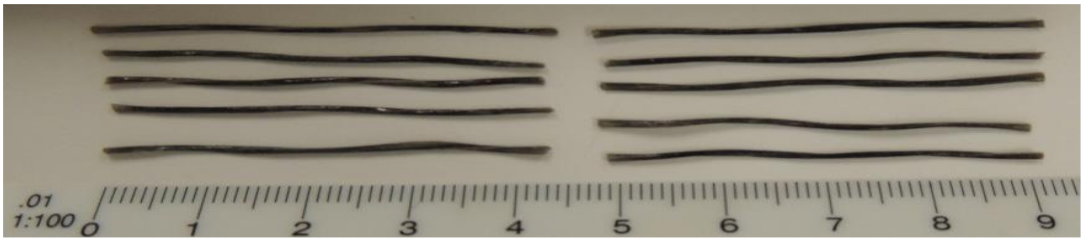

Figure 2. Length of Basalt Macro-Fibers

Table 1 Properties of BMF

Diameter (µm)	660
Length (mm)	40 - 45
Density (gm/cc)	2
Specific Gravity (g/cm^3)	2.68
Water Absorption	None
Tensile Strength (MPa)	1080
E modulus (Gpa)	90
Alkaline Resistance	Excellent
Thermal Operating Range (c)	-260 to +700
Electrical Conductivity	None
Resistance to Corrosion	Non Corrosive

3.1.2 Fiber Reinforced Polymer Reinforcing Bars

FRP reinforcing bars are an alternative material to traditional steel reinforcing bars. They are constructed from a combination of fibers roving and resin materials. The fibers are made from different natural materials like carbon, glass, aramid and basalt. The nature of its raw materials making FRP as a corrosion resistant and lightweight material.

In this research basalt FRP (BFRP) and glass FRP (GFRP) reinforcing bars showed in Figures 3 and 4 respectively were used in two different sizes, 10 mm diameter and 12 mm diameter. Table 2 shows specifications of BFRP and GFRP from manufacturers (Magmatech, 2016; MateenBar, 2016).

Figure 3. BFRP Reinforcing Bars

Figure 4. GFRP Reinforcing Bars

Table 2 Properties of FRP Reinforcing Bars

Type of Reinforcement	Yield Strength (MPa)	Modulus of elasticity (GPa)	Surface
GFRP	1060	45	Ribbed
BFRP	1168	50	Sand Coated

3.1.3 Concrete Mix Design

The concrete mix used in this research were prepared in accordance with ASTM C 192, and designed to achieve target compressive strength of 40 MPa at 28 days. CHRYSO Fluid CQ 515 is the only added additive to the concrete mix to achieve the acceptable concrete flowability and workability. Coarse aggregate particles retained on 4.75 mm (No.4) sieve, and fine aggregate particles passing 4.75 mm (No.4) sieve and retaining on 0.075 mm (No.200) sieve. Table 3 shows quantities of each content used in a concrete mix in this study.

Table 3 Concrete Mix Design

Sample	Portland Cement (kg/m^3)	Water (kg/m^3)	Fine Aggregate (kg/m^3)	Coarse Aggregate from Gabbro (kg/m^3)	BMF Volume Fraction (%)	BMF (kg/m^3)
CM1	365	180	730	1080	0%	0
CM2	365	180	730	1080	0.5%	9.5
CM3	365	180	730	1080	1%	19
CM4	365	180	730	1080	2%	38

3.2 EXPERIMENTAL PROGRAM

This section is about the experimental program of testing of materials used in this study. Before testing of the FRP reinforced one-way concrete slabs, materials used to prepare these one-way concrete slabs samples should be tested to verify their properties. Testing procedures of GFRP reinforcing bar tensile strength, concrete compressive strength and concrete flexural tensile strength will be explained. After that design, casting and testing procedures of the one-way concrete slabs will be explained in this Chapter. The experimental program contains two main levels:

1- Materials characterization tests to study the properties of materials used in this study. It includes the tensile test for FRP reinforcing bars, and compressive strength and flexural tensile tests for FRC.

2- Large-scale one-way concrete slab test in order to study the flexural behavior of FRP reinforced one-way concrete slabs.

3.2.1 Tensile Strength of FRP Bars

This test is used to determine the tensile strength and modulus of elasticity of FRP reinforcing bars. According to ASTM D7205, the tensile strength of FRP bars is performed by holding an FRP bar by the tensile test machine after putting it inside a steel cylinder filled with poly-vinyl chloride (PVC) as showed in Figures 5 and 6, That is because FRP bars is anisotropic material where they are very weak in compression in the transverse direction. (ASTM D7205/D7205M-06, 2011).

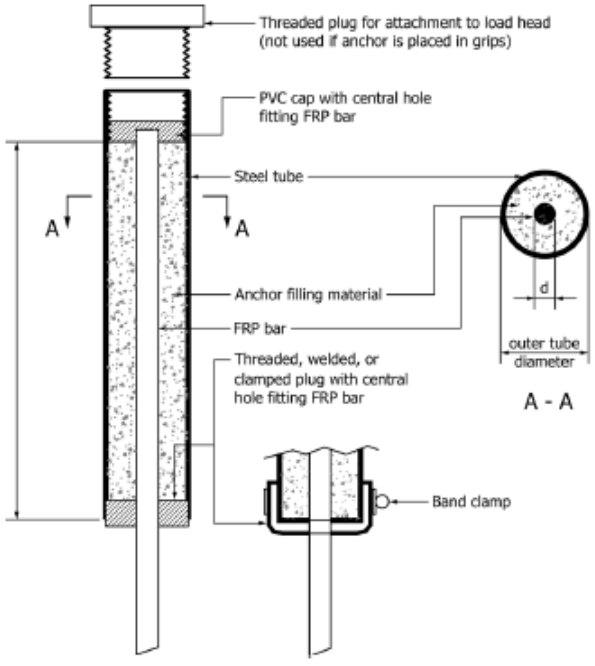

Figure 5. Handling System of FRP Reinforcing Bars for Tensile Strength Test (ASTM D7205/D7205M-06, 2011)

Figure 6. FRP Reinforcing Bars under Tensile Strength Test

3.2.2 Concrete Compressive Strength

This test is necessary to come up with the concrete compressive strength. According to ASTM C39 procedures, three-cylinder concrete samples with dimensions of 150 mm in diameter and 300 mm in height from each mix were tested, using the concrete compressive machine test as shown in Figures 7 and 8. The compressive strength of a concrete mix is the average result of these three samples after 28 days of curing. Cylinder cappers are capping the sample to get the best accurate results by having a perfectly perpendicular

surface to the axis of the cylinder in order to improve the smoothness and reduce the possibility of eccentric loading (ASTM C39/C39M-12a, 2012).

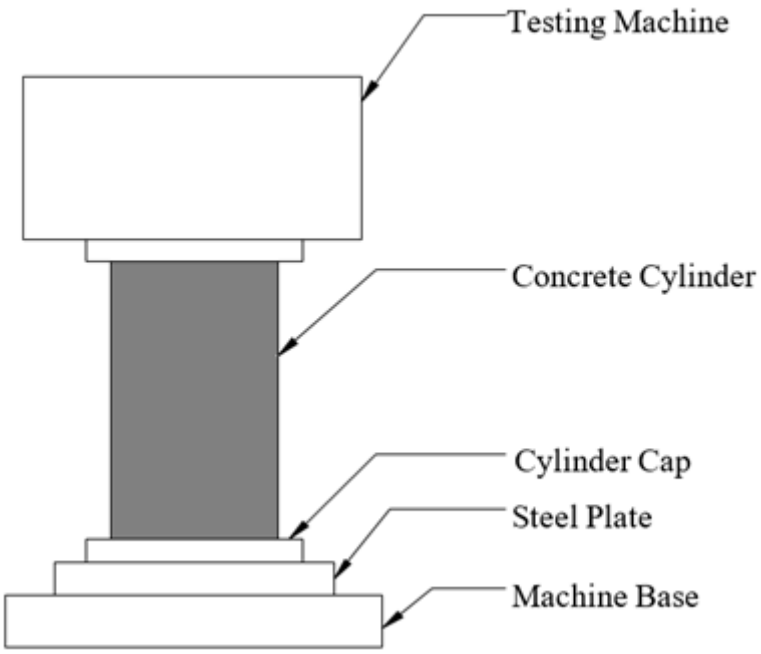

Figure 7. Concrete Compressive Strength Test Setup

Figure 8. Concrete Cylindrical Samples Before, During and After Testing

3.2.3 Concrete Flexural Tensile Strength

This test is implemented to come up with the concrete flexural tensile strength. According to ASTM C78 procedures, three 100 mm in depth, 100 mm in width and 500 mm in long prisms samples of concrete from each mix will be tested, using concrete flexural tensile machine test as shown in Figures 9 and 10. The flexural tensile strength of a concrete mix is the average result of these three samples after 28 days of curing. This test was implemented on a simply supported prism, by applying two points load on it. The spacing between a support and the nearest point load should be 100 mm and also the spacing between two points load (ASTM C78, 2002).

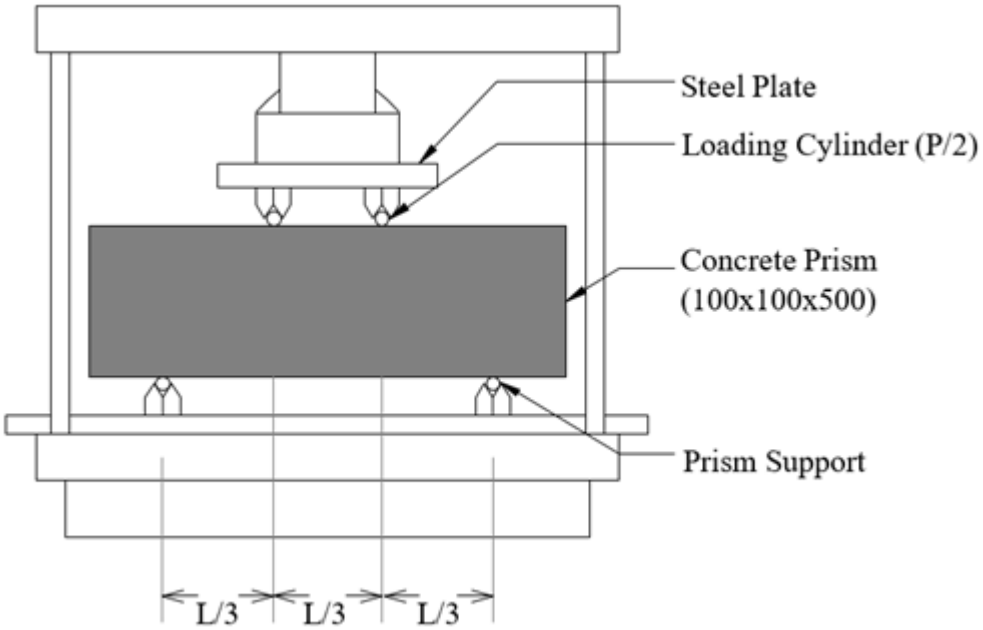

Figure 9. Flexural Tensile Strength Test Setup

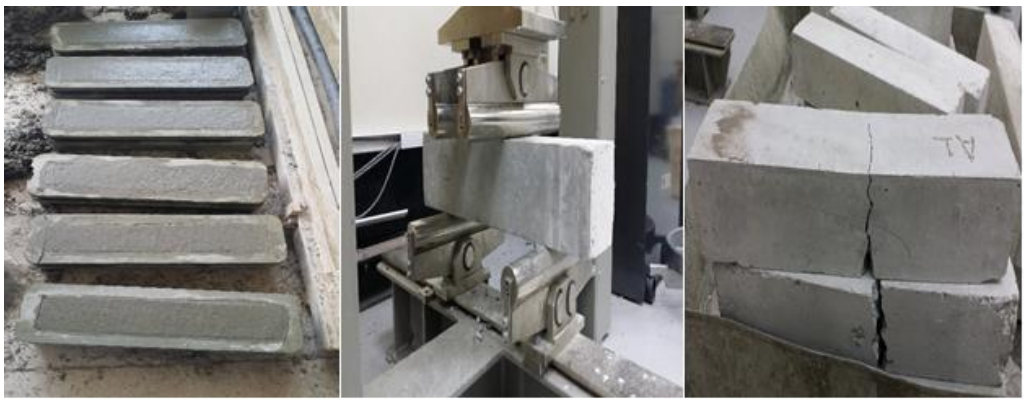

Figure 10. Concrete Prism Samples Before, During and After Testing

3.2.4 One-Way Concrete Slabs Design, Preparation and Testing

3.2.4.1 FRP Reinforced One-Way Concrete Slabs Design

FRP reinforced one-way concrete slabs were designed according to ACI 440.1R following the ultimate strength approach. It is important to know that FRP reinforced concrete one-way slabs should be designed to be a compression controlled not a tension controlled as in SRC one-way slabs. That is because FRP reinforcing bars are perfectly brittle materials and do not have ductility like steel reinforcing bars. All samples were designed to be either balanced reinforced ($\rho_f = 1.4\rho_{fb}$) or over-reinforced ($\rho_f = 2.8\rho_{fb}$), so the first step is finding ρ_{fb} using Equation 1 (ACI 440.1R-15):

$$\rho_{fb} = 0.85\beta_1 \frac{f'_c}{f_{fu}} \frac{E_f \varepsilon_{cu}}{E_f \varepsilon_{cu} + f_{fu}} \qquad \text{Equation 1}$$

Where, ρ_{fb} is the balanced reinforced ratio. β_1 is a factor relating depth of equivalent rectangular compressive stress block to neutral axis depth ($\beta_1 = 0.88$). f'_c is the specified compressive strength of concrete. f_{fu} is the design tensile strength of FRP, considering reductions for service environment (calculated by Equation 2 from ACI 440.1R). E_f is the design or guaranteed modulus of elasticity of FRP reinforcing bars defined as mean modulus of test specimens ($E_f = 50\text{GPa}$). And ε_{cu} is the maximum usable strain at extreme concrete compression fiber ($\varepsilon_{cu} = 0.003$).

$$f_{fu} = C_E f^*_{fu} \qquad \text{Equation 2}$$

Where, C_E is the environmental reduction factor and f^*_{fu} is the guaranteed tensile strength of an FRP reinforcing bar. Since there is no data for the environmental reduction factor of BFRP reinforcing bars, the design tensile strength will be 1000 MPa.

$$\therefore \rho_{fb} = 0.85 \times 0.88 \times \frac{40}{1000} \times \frac{50{,}000 \times 0.003}{50{,}000 \times 0.003 + 1000} = 3.9 \times 10^{-3}$$

After calculating the balanced reinforced ratio, the reinforcing area can be calculated using Equations 3 and 4:

$$\rho_{1.4} = 1.4\rho_{fb} \qquad \text{Equation 3}$$

$$\rho_{2.8} = 2.8\rho_{fb} \qquad \text{Equation 4}$$

Where, $\rho_{1.4}$ is the balanced reinforced ratio used in this study and $\rho_{2.8}$ is the over-reinforced ratio used in this study.

$$\therefore \rho_{1.4} = 1.4 \times 3.9 \times 10^{-3} = 5.5 \times 10^{-3}$$

$$\rho_{2.8} = 2.8 \times 3.9 \times 10^{-3} = 10.92 \times 10^{-3}$$

Then by using Equation 5 from ACI 440.1R the required area of FRP reinforcing bars can be defined:

$$A_{fr} = \rho_f bd \qquad \text{Equation 5}$$

Where, A_{fr} is the required area of FRP reinforcing bars, b is the one-way concrete slab sample's width ($b = 500\text{mm}$) and d is the one-way concrete slab's effective depth (calculated by Equation 6).

$$d = h - \text{clear cover} - \text{stirrup diameter} - \text{bar diameter}/2 \qquad \text{Equation 6}$$

Where h is the one-way concrete slab sample's depth ($h = 175\text{mm}$).

$$\therefore d = 175 - 25 - 8 - \frac{10}{2} = 137\text{mm}$$

$$\therefore A_{1.4} = 5.5 \times 10^{-3} \times 500 \times 137 = 376.75\text{mm}^2$$

$$A_{2.8} = 10.92 \times 10^{-3} \times 500 \times 137 = 748.02\text{mm}^2$$

The equivalent reinforcing for balanced reinforced one-way concrete slab samples is 2ϕ12 and 2ϕ10 (Figure 11). And 4ϕ12 and 4ϕ10 for over-reinforced one-way concrete slab samples (Figure 12).

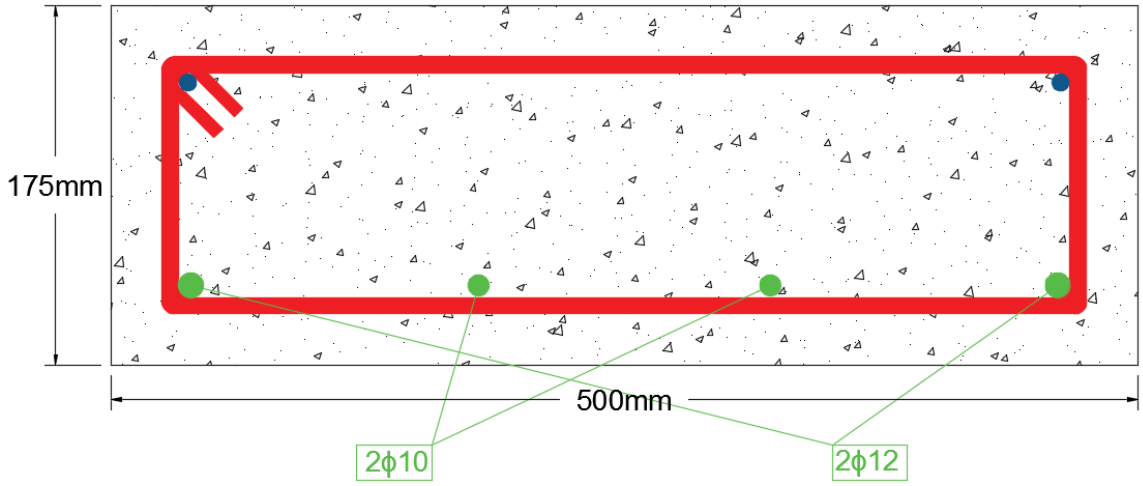

Figure 11. Cross Section of Balanced Reinforced One-Way Concrete Slabs Sample

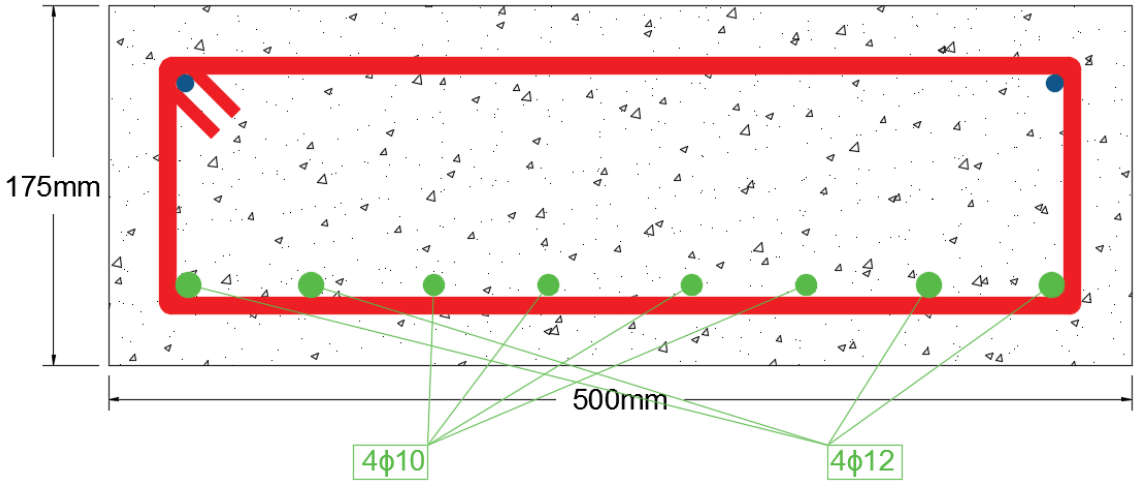

Figure 12. Cross Section of Over-Reinforced One-Way Concrete Slabs Sample

3.2.4.2 Preparation and Fabrication of One-Way Concrete Slabs Samples

The first step in concrete casting is the shuttering work, in order to prepare molds using plywood as a raw material. Mold's inner dimensions should be equivalent to one-way concrete slab specimens' dimensions. After that FRP reinforcing bars to be cut in the same length of specimens, in same quantities mentioned in the design section with two 8 mm steel reinforcing bars in the top section. All reinforcing bars were surrounded by steel stirrups. Concrete biscuits with a height equivalent to concrete clear cover were connected to the bar cage to guaranteed the concrete clear cover. The final stage before mixing the concrete was connecting four strain gauges to the FRP reinforcing bars using superglue. Then adding steel hooks to carry the samples. Molds were cleaned well and sprayed by oil from inside before casting in order to open them easily after drying. Figure 13 shows the steps of preparation of molds and bar cages.

After preparation of the mold and the bar cage, concrete components were mixed together by concrete mixer as shown in Figure 14. Then cylinders and prisms molds were filled with fresh concrete. Concrete mix were cast into the one-way concrete slabs' molds in two layers. Each layer was compacted well by using a vibrator machine and the top surface was prepared to be smooth as shown in Figure 15. The final stage was curing all samples by water for 28 days in order to compensate the evaporated water by covering the one-way slab samples by wet pieces of sackcloth as shown in Figure 16.

a) Concrete Biscuits

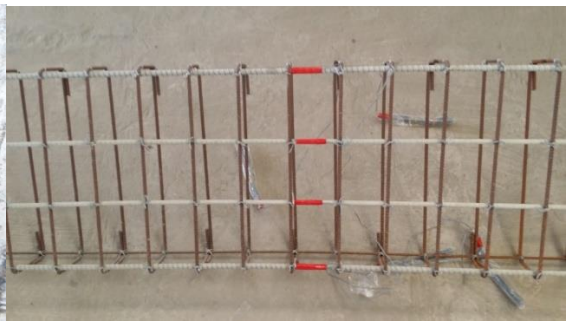

b) Bar Strain Gauges

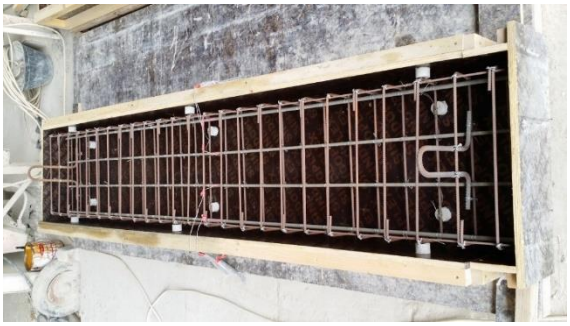

c) Cage inside the Mold

Figure 13. Preparation of Molds and Bar Cages

a) Putting Water

b) Putting Fine Aggregate

c) Putting Coarse Aggregate

d) Putting Cement

e) Putting BMF

Figure 14. Steps of Concrete Mixing

a) Cylinders and Prisms b) Casting Concrete

c) Using Vibrator Machine d) Preparing Concrete Top Surface

Figure 15. Steps of Casting of One-Way Concrete Slabs

Figure 16. Curing of One-Way Concrete Slabs

3.2.4.3 Flexural Test for One-Way Concrete Slabs

Using the Instron 1500HDX static hydraulic universal test machine, each one-way concrete slab sample was placed as a simply supported one-way slab. Supports were placed 175 mm away from the one-way concrete slab edge. The applied load from the universal test machine was divided to two points load, with 600 mm distance between the two points load, as shown in Figures 17 and 18. Two linear variable differential transformers (LVDT) were placed on sides of mid-span to measure the deflection, and two concrete strain gauges were placed on the top surface of the one-way concrete slab sample at equal spacing on the mid-span (Figure 19). All LVDTs and strain gauges were connected to a data logger by electrical wires, and the data logger was connected to a computer to show results readings as shown in Figure 20.

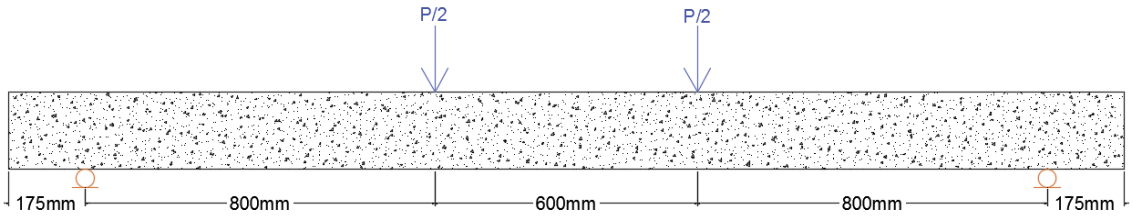

Figure 17. One-Way Concrete Slab Testing Setup

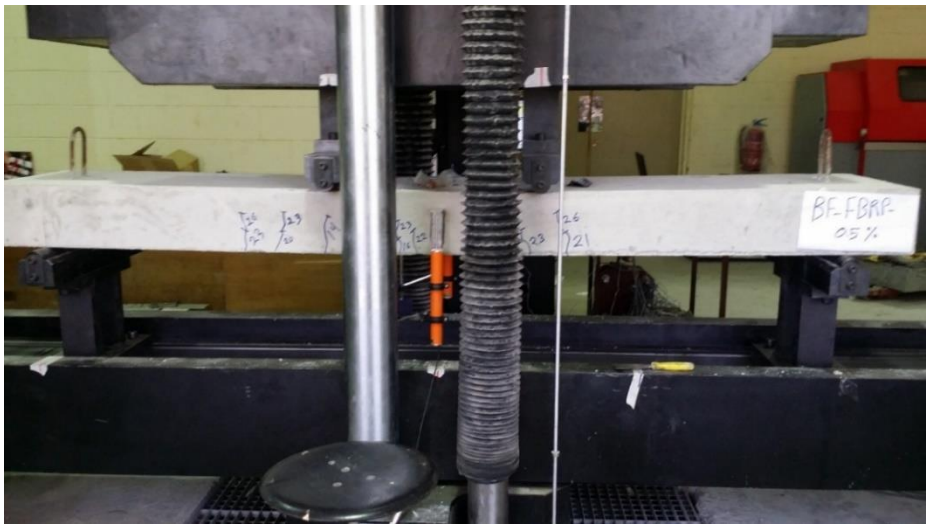

Figure 18. One-Way Concrete Slab during Test

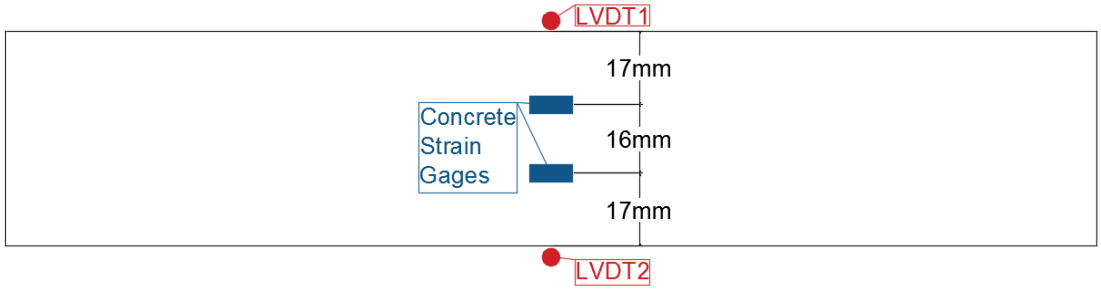

Figure 19. Top View of One-Way Concrete Slab Showing Locations of LVDTs and Concrete Strain Gauges

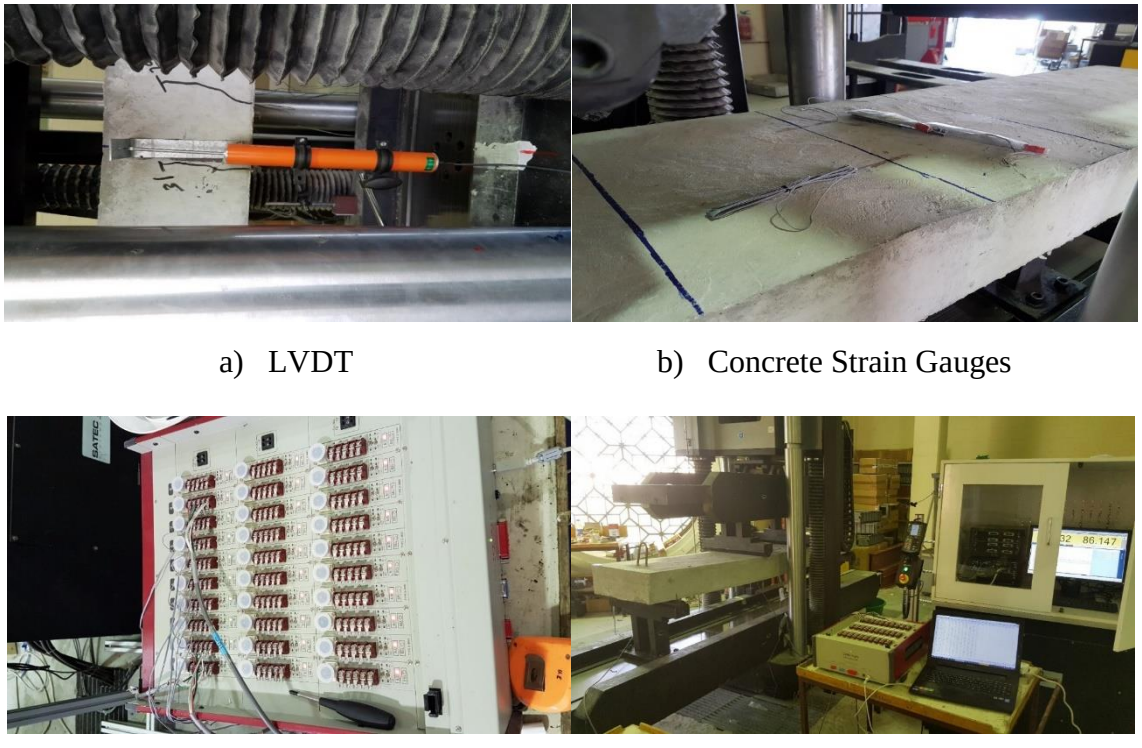

a) LVDT

b) Concrete Strain Gauges

c) Data Logger

d) Large-Scale One-Way Slab Test Setup

Figure 20. One-Way Concrete Slab Test Set-Up

CHAPTER 4: TESTING RESULTS AND DISCUSSIONS

4.1 TEST MATRIX

Test matrix used in this study covered the following three main parameters, to give the best understanding and clearest picture of the behavior of RC structures with FRP reinforcing bars and mixed with BMF:

1- Reinforcement Ratio: Two different reinforcement ratios were used to show the behaviors of one-way concrete slabs: the balanced reinforced ratio ($\rho_f = 1.4\rho_{fb}$) and the over-reinforced ratio ($\rho_f = 2.8\rho_{fb}$).

2- Type of Reinforcing Bars: Two different FRP reinforcing bars were used (Basalt FRP and Glass FRP bars).

3- BMF Volume Fraction: Four different volume fractions of BMF were used in this study (0%, 0.5%, 1% and 2%).

Test matrix was set to study each parameter and its influence on other parameters as specified in Table 4.

Table 4 Testing Matrix of Large-Scale One-Way Slabs

Slab No.	Reinforcement Ratio	Reinforcement Type	BMF Volume Fraction	Slab Description
A1	$1.4\rho_{fb}$	Basalt FRP	0%	FB-BFRP-0%
A2	$1.4\rho_{fb}$	Basalt FRP	0.5%	FB-BFRP-0.5%
A3	$1.4\rho_{fb}$	Basalt FRP	2%	FB-BFRP-2%
A4	$2.8\rho_{fb}$	Basalt FRP	0%	FC-BFRP-0%
A5	$2.8\rho_{fb}$	Basalt FRP	0.5%	FC-BFRP-0.5%
A6	$2.8\rho_{fb}$	Basalt FRP	1%	FC-BFRP-1%
A7	$2.8\rho_{fb}$	Basalt FRP	2%	FC-BFRP-2%
A8	$1.4\rho_{fb}$	Glass FRP	0%	FB-GFRP-0%
A9	$1.4\rho_{fb}$	Glass FRP	1%	FB-GFRP-1%
A10	$1.4\rho_{fb}$	Glass FRP	2%	FB-GFRP-2%
A11	$2.8\rho_{fb}$	Glass FRP	0%	FC-GFRP-0%
A12	$2.8\rho_{fb}$	Glass FRP	2%	FC-GFRP-2%

4.2 TENSILE STRENGTH OF FRP BARS RESULTS

The tensile strength test of GFRP reinforcing bars was continued until GFRP reinforcing bars were failed as shown in Figure 21. Test Results showed that the tensile strength of GFRP reinforcing bars was 1020 MPa and for the nominal modulus of elasticity

was 45 GPa, as illustrated in Figure 22. For BFRP reinforcing bars the nominal tensile strength and nominal modulus of elasticity have been taken from the manufacturer data sheet as showed in Table 2.

Figure 21. GFRP Reinforcing Bars after Failure

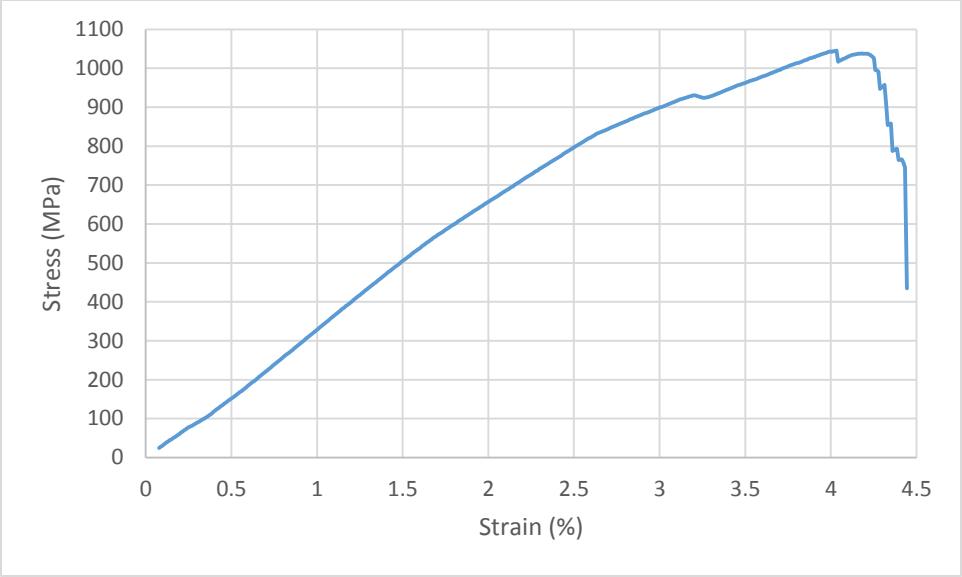

Figure 22. Stress-Strain Diagram of GFRP Reinforcing Bars

4.3 CONCRETE COMPRESSIVE STRENGTH RESULTS

The concrete compressive strength test is obtained after 28 days of curing in order to achieve the ultimate strength of the concrete. Three cylinders were taken out from each one-way concrete slab sample, and the average of the results was calculated as shown in Table 5. The only difference between concrete mixes is the volume fraction of BMF. To show their effects on concrete compressive strength, average values of equivalent samples were calculated and showed in Figure 23. Test results showed that the volume fraction of BMF has little to no effect on the concrete compressive strength, because the BMF is weak in compression. While in steel fiber reinforced concrete (SFRC), the compressive strength increases with increasing the volume fraction of SMF. This enhancing of concrete

compressive strength with SMF, is due to the ability of steel to resist compression forces (Holschemacher, 2010; Mohammadi, 2009; Katzer, 2012).

Table 5 Concrete Compressive Strength Values

Sample	Description	BMF Volume Fraction (%)	Concrete Compressive Strength (MPa)			
			Cylinder 1	Cylinder 2	Cylinder 3	Average
A1	FB-BFRP-0%	0	38.61	39.1	40.22	39.31
A2	FB-BFRP-0.5%	0.5	39.71	40.4	39.21	39.77
A3	FB-BFRP-2%	2	35.61	39.48	34.57	36.55
A4	FC-BFRP-0%	0	36.12	37.8	40.24	38.05
A5	FC-BFRP-0.5%	0.5	39.94	39.71	41.81	40.49
A6	FC-BFRP-1%	1	38.54	39.92	39.03	39.16
A7	FC-BFRP-2%	2	42.76	43.15	41.65	42.52
A8	FB-GFRP-0%	0	42.64	42.94	42.27	42.62
A9	FB-GFRP-1%	1	46.13	44.48	46.54	45.72
A10	FB-GFRP-2%	2	42.56	40.16	41.81	41.51
A11	FC-GFRP-0%	0	45.16	45.28	33.15*	45.22
A12	FC-GFRP-2%	2	41.23	41.08	37.97	40.09

* Outlier value

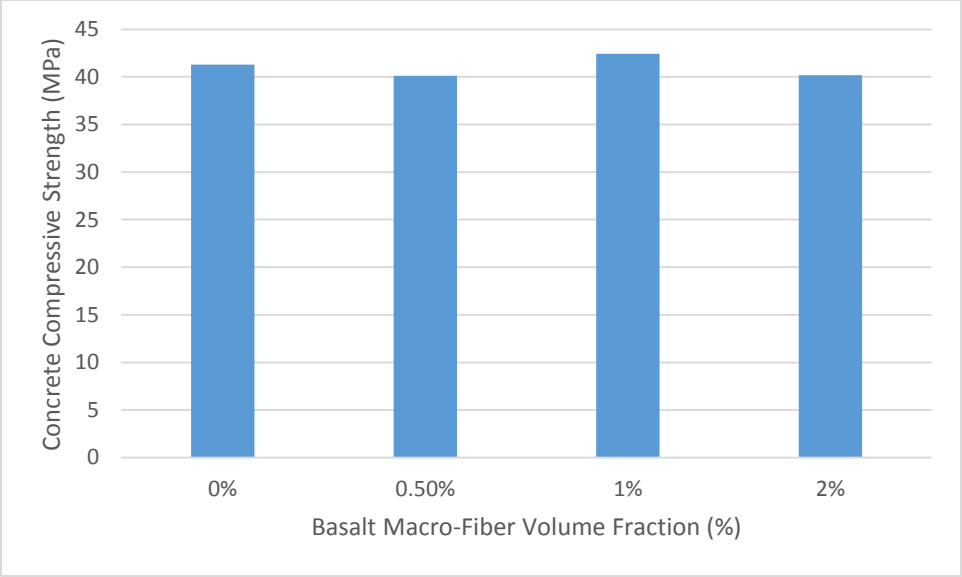

Figure 23. Concrete Compressive Strength with Different Volume Fraction Ratios of BMF

4.4 CONCRETE FLEXURAL TENSILE STRENGTH RESULTS

Prisms were tested to find the FRC tensile strength. Table 6 shows values and the average values of prisms' tensile strength. Again to show the effect of BMF volume fraction, average values of equivalent samples in BMF volume fraction were calculated and showed in Figure 24. From these values, it is clear that the concrete flexural tensile strength was enhanced by increasing of BMF volume fraction. This because these macro-fibers are acting as mini reinforcing bars spreading all over the concrete matrix. BMF are spreading better and covering more areas of the concrete matrix with more percentage of their volume fraction. This clear from the increasing of concrete flexural tensile strength with the increasing of BMF volume fraction. Because in samples with the low volume

fraction of BMF, BMF is not spreading well and do not cover more areas as in samples with more volume fraction of BMF.

Table 6 Concrete Flexural Tensile Strength Values

Sample	Description	BMF Volume Fraction (%)	Concrete Tensile Strength (MPa)			
			Prism 1	Prism 2	Prism 3	Average
A1	FB-BFRP-0%	0	3.84	3.73	2.8*	3.79
A2	FB-BFRP-0.5%	0.5	4.45	3.37*	4.62	4.54
A3	FB-BFRP-2%	2	5.21	5.39	5.14	5.25
A4	FC-BFRP-0%	0	3.03	3.39	3.66	3.36
A5	FC-BFRP-0.5%	0.5	4.39	3.89*	4.51	4.45
A6	FC-BFRP-1%	1	4.37	4.18	4.72	4.42
A7	FC-BFRP-2%	2	7.6*	5.11	5.24	5.18
A8	FB-GFRP-0%	0	4.33	4.17	4.3	4.27
A9	FB-GFRP-1%	1	5.36	4.91	5.65	5.31
A10	FB-GFRP-2%	2	5.4	5.31	5.15	5.29
A11	FC-GFRP-2%	0	4.05	3.06*	3.6	3.83
A12	FC-GFRP-2%	2	5.37	4.86	5.32	5.18

* Outlier values

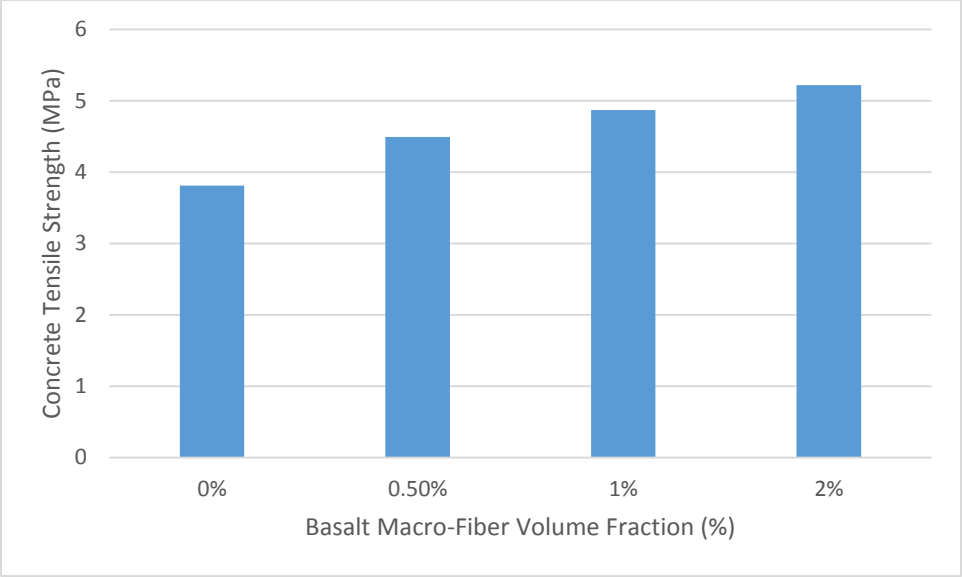

Figure 24. Concrete Flexural Tensile Strength with Different Volume Fraction Ratios of BMF

4.5 RESULTS OF FLEXURAL TEST FOR ONE-WAY CONCRETE SLABS

4.5.1 Mid-Span Deflection

As mentioned in the experimental procedures, deflection was measured at two points at sides of the mid-span using LVDTs. The deflection behavior was approximately similar in all one-way concrete slab specimens. It started linear with high slope value in the precracking stage. The behavior was approximately similar in all specimens in the precracking stage because the tensile stress is resisted by the concrete only in this stage. After reaching the cracking load, the slope is decreased due to decreasing of the stiffness, but the curve still linear with different slopes between one-way concrete slabs because FRP reinforcing bars are resisting the tensile stress after the cracking load. It was noticed that

the cracking moment is improved in the presence of BMF, because BMF works as mini reinforcing bars inside the concrete matrix. Table 7 shows values of cracking loads and moments, ultimate loads and moments and deflection at cracking and at the failure of each one-way concrete slabs sample.

Table 7 Loads, Moments & Deflection Values due to Experiments

Slab	P_{cr} (kN)	M_{cr} (kN.m)	P_u (kN)	M_u (kN.m)	δ_{cr} (mm)	δ_f (mm)
A1 (FB-BFRP-0%)	11.89	5.13	96.46	38.58	1.48	86.46
A2 (FB-BFRP-0.5%)	14.06	7.14	100.57	40.23	0.99	84.27
A3 (FB-BFRP-2%)	20.71	9.96	110.01	44	1.61	88.97
A4 (FC-BFRP-0%)	10.07	6.52	110.93	44.37	2.45	58.66
A5 (FC-BFRP-0.5%)	14.77	7.62	111.11	44.44	1.62	66.94
A6 (FC-BFRP-1%)	18.13	9.06	133.39	53.36	1.31	70.32
A7 (FC-BFRP-2%)	21.72	11.26	155.19	62.08	1.59	82.09
A8 (FB-GFRP-0%)	9.42	4.23	74.95	29.98	0.64	66.58
A9 (FB-GFRP-1%)	17.11	7.6	88.83	35.53	1.46	73.51
A10 (FB-GFRP-2%)	19.52	8.95	93.82	37.53	2.92	79.93
A11 (FC-GFRP-0%)	18.89	7.56	124.65	49.86	2.55	61.71
A12 (FC-GFRP-2%)	22.03	11.58	164.41	65.76	1.65	68.65

The main objective of the experimental part of this study is to reach for experimentally-driven conclusive remarks about the effect of following two parameters on the flexural behavior of RC beams: i.) reinforcement ratio; ii.) Type of reinforcement, and iii) Volume fraction ratio of BMF. A detailed discussion about the effect of the above-mentioned parameters is shown below.

4.5.1.1 Effecting of Reinforcement Ratio on Deflection at Mid-Span

One-way concrete slabs with two different reinforcement ratios and the same type of reinforcement and BMF volume fraction ratio were compared in order to know how reinforcement ratio is affecting the behavior of one-way concrete slab deflection. Figure 25 shows load-deflection relationships for one-way slabs A1 and A4. Cracking moments were approximately the same, because cracking moment depends mainly on concrete. After cracking, behaviors were changed. From slopes, it is clear that A4 had more stiffness than A1. It reached failure point with more resisted load by 15% and less deflection by approximately the half. Because of increasing reinforcement bars, the ability of the element to resist more loads was enhanced. Behaviors of both one-way concrete slabs were brittle because of the brittle nature of BFRP reinforcing bars and concrete mix.

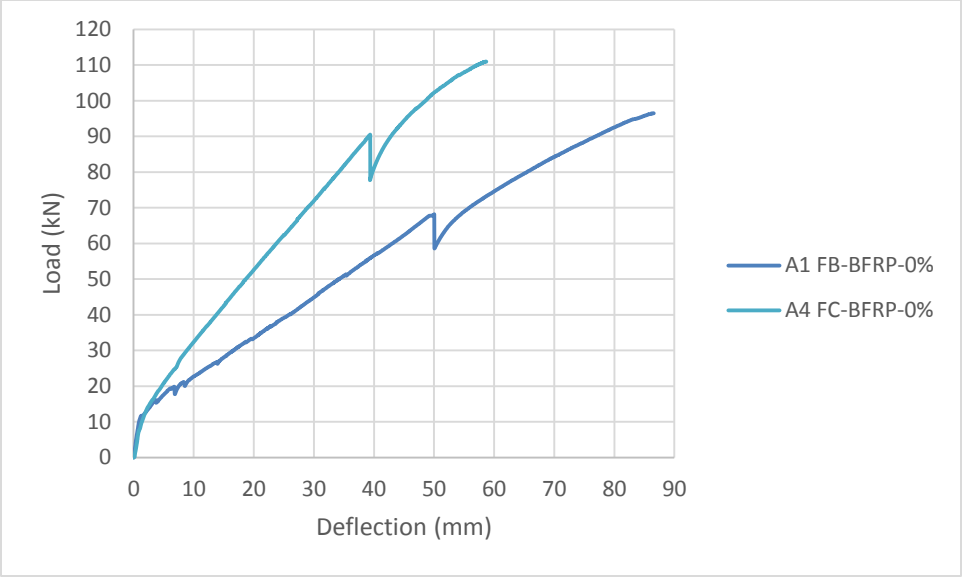

Figure 25. A1 & A4 Load - Deflection Relationships

Figure 26 shows load-deflection relationships for one-way slabs A2 and A5. Cracking moments were approximately the same in both slabs. But more than cracking loads of A1 and A4, because of adding BMF. Behaviors of deflection with respect to load were generally the same of behaviors of A1 and A4. BMF give some ductile behavior before failure with a longer period in A5. A5 was more stiffness than A2, and reached the failure point with more load resisted by 10.48% and less deflection by 25.89%.

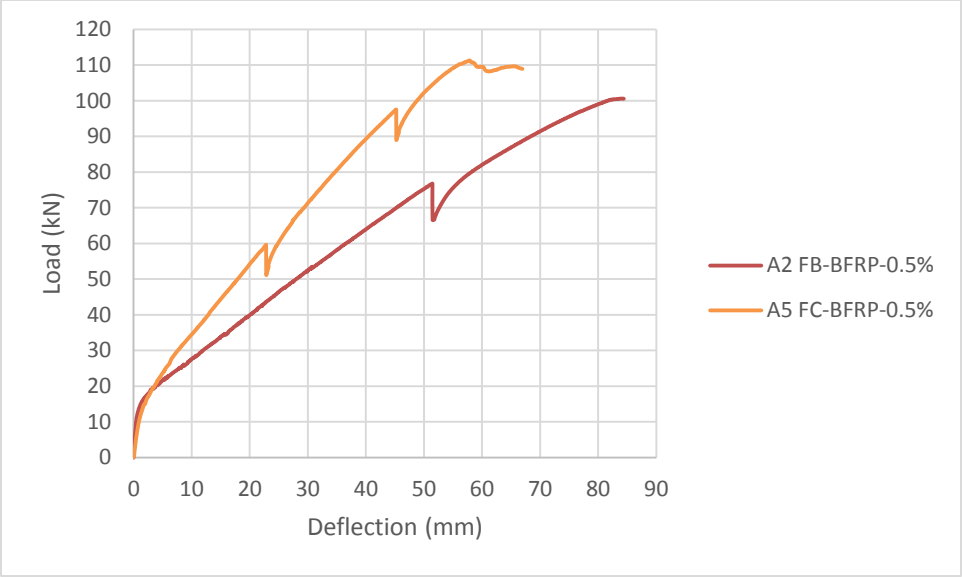

Figure 26. A2 & A5 Load - Deflection Relationships

Load-deflection relationships of one-way concrete slabs A3 and A7 were shown in Figure 27. Cracking moments were increased in both of them by 47.3% from A2 to A3 and 47.05% from A5 to A7, which shows that the BMF volume fraction is a key factor of cracking moment. After cracking, behaviors were brittle in both one-way concrete slabs. However, before failure, they acted in a ductile manner and that was because of the effect of BMF that gives ductility to the concrete mix. Again A7 had more stiffness by 41.07% and less deflection by 8.38% compared to A3.

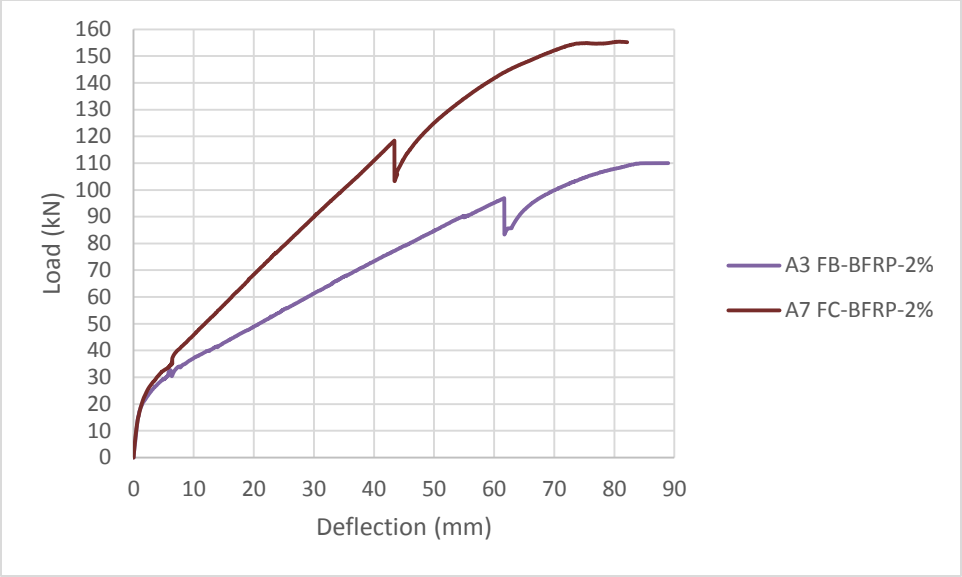

Figure 27. A3 & A7 Load - Deflection Relationships

In BFRP reinforced concrete one-way concrete slabs, the difference of the ultimate load between over-reinforced and balanced reinforced slabs increased rapidly in slabs with 2% BMF volume fraction than other samples. Because the presence of BMF in over-reinforced concrete gives the concrete more ability to resist more load by acting as additional mini reinforcing bars distributed and covering most of the concrete matrix. On the other hand, deflection differences were decreased between over-reinforced and balanced reinforced ratios with increasing BMF volume fraction. This decreasing belongs to the ductility of the concrete gained by BMF presence, which gives the concrete an ability to deflect more under its ultimate load before failure. This is the ideal alternative to steel reinforcing bars ductility that gives a chance to escape before collapsing, and this advantage is not in BFRP reinforced concrete structures.

Figure 28 shows load-deflection relationships of one-way concrete slabs A8 and A11. Cracking moments were approximately doubled with doubling the reinforcement ratio, and behaviors were brittle. Again the main effecting factor on stiffness was the reinforcement ratio, where the ultimate load was increased by 66.31% and deflection was decreased by 7.89% with the over-reinforced one-way concrete slab.

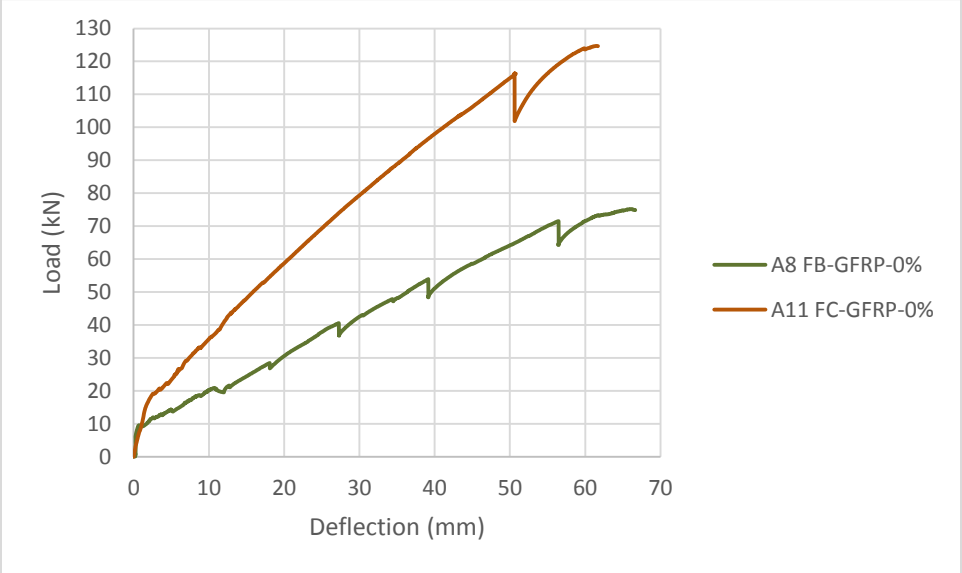

Figure 28. A8 & A11 Load - Deflection Relationships

Behaviors of one-way concrete slabs A10 and A12 showed in Figure 29, show that the cracking moment was more in A12 by 12.86% than cracking moment in A10 and by 16.62% than cracking moment in A11. That shows that both GFRP reinforcement ratio and

BMF volume fraction affect the cracking point by increasing it with their increase. In addition, 2% BMF volume fraction with over-reinforced ratio give the one-way concrete slab an obvious ductile manner. The over-reinforced one-way concrete slab resisted more load than the balanced reinforced one by 75.24% and deflected less by 16.43%.

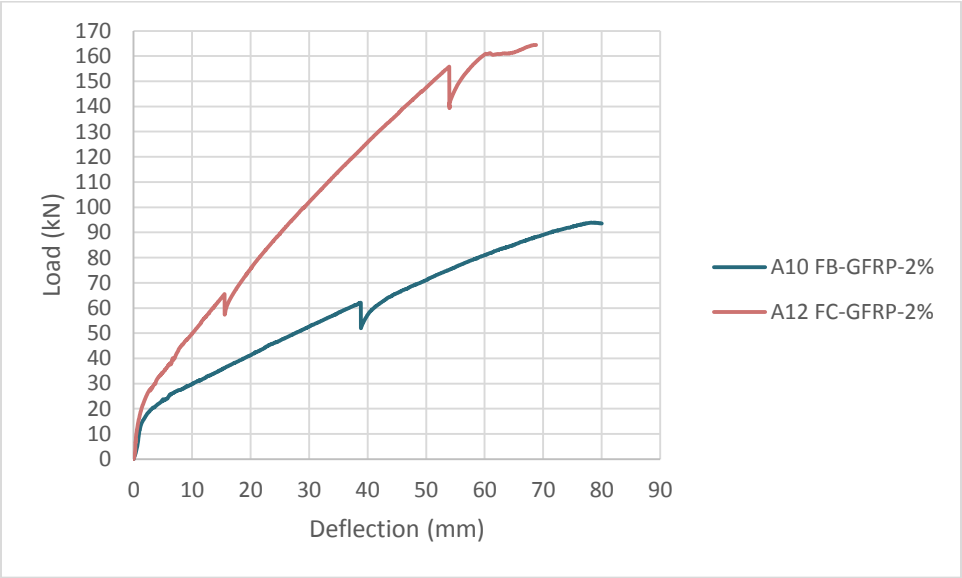

Figure 29. A10 & A12 Load - Deflection Relationships

With BFRP reinforcing bars, one-way concrete slabs acted in a brittle manner until failure because of the brittle nature of BFRP reinforcing bars and concrete mix. But with adding BMF, one-way concrete slabs gained some ductility. That shows that BMF give ductility to the concrete mix. But with GFRP reinforcing bars, one-way concrete slabs had

more ductility than in BFRP reinforcing bars. Also, the reinforcement ratio was an effective factor on the cracking moment, this because of the ribbed surface of GFRP reinforcing bars that makes the surrounding concrete matrix does not slip easily like in sand coated surface of BFRP reinforcing bars. As a result, the bonding force was increased rapidly with the increase of the reinforcement ratio. It can be concluded that the major factors affecting the cracking moment by reinforcement ratio was the bonding force between reinforcing bars and surrounding concrete and the specifications of concrete matrix. The effecting of the ribbed surface on the bonding force resulted in a big difference in the ultimate load between over-reinforced and balanced reinforced one-way concrete slabs, where doubling the reinforcement made an immense effect on bonding force and increased the ultimate strength more than the double. Where in the sand coated surface increasing in the stiffness was less. On the other hand, ductility was improved by increasing BMF volume fraction.

4.5.1.2 Effecting of Type of Reinforcement on Deflection at Mid-Span

Figure 30 compares behaviors of deflection with respect to load acting on one-way concrete slabs A1 and A8. Cracking moments were approximately the same. The ultimate moment was larger in A1 by 28.7% than A8 and the deflection was also larger by 29.86% in A1.

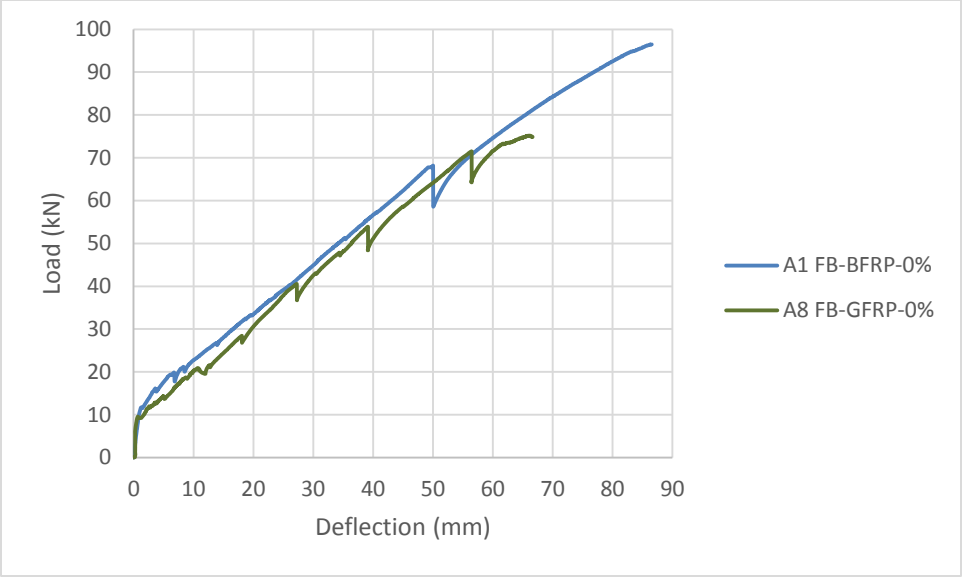

Figure 30. A1 & A8 Load - Deflection Relationships

In Figure 31 one-way concrete slabs A3 and A10 were compared. Cracking moments values were approximately equal, but stiffness in A3 was quite better than in A10. Also, ultimate load in A3 was greater by 17.26% than in A10, and so deflection at failure was also more in A3 than A10 by 11.31%.

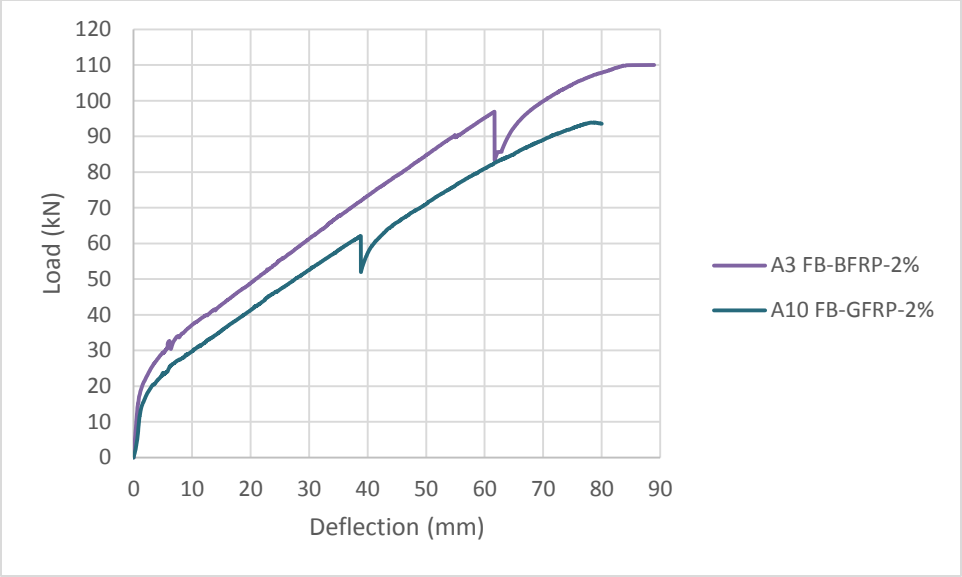

Figure 31. A3 & A10 Load - Deflection Relationships

From the comparison of one-way concrete slabs A4 and A11 in Figure 32. It was illustrated that the cracking moment of A11 was grater by 87.59% than the cracking moment of A4, and the stiffness of A11 was quite little more than the stiffness of A4. As a result of that, ultimate load of A11 was greater by 12.37% than ultimate load of A4 and failure deflection in A11 was more than in A4 by 5.2%.

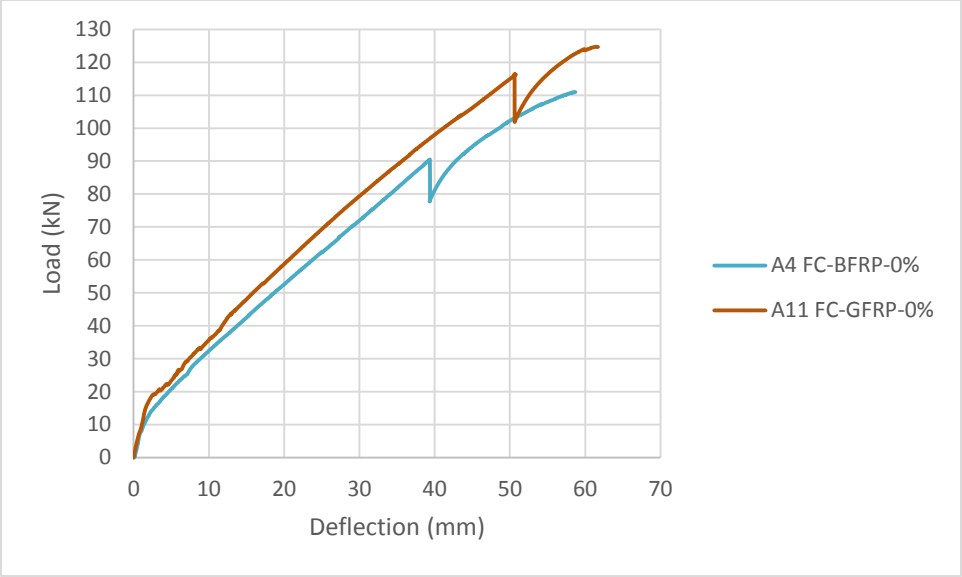

Figure 32. A4 & A11 Load - Deflection Relationships

Figure 33 shows deflection behaviors related to load in one-way concrete slabs A7 and A12. Cracking moments of both of them were approximately equal, but after cracking point A12 was more stiffness than A7. The ultimate load of A12 was more than the ultimate load of A7 by 5.94%. On the other hand, deflection of failure in A7 was more by 19.58% than in A12. Both one-way concrete slabs behaved in a ductile manner before failure, and that because the BMF volume fraction enhances concrete ductility.

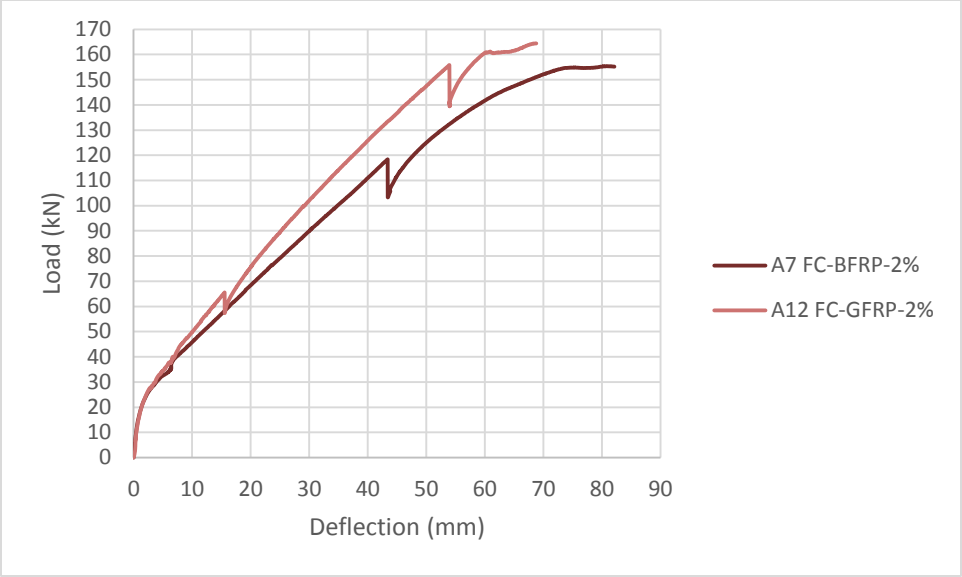

Figure 33. A7 & A12 Load - Deflection Relationships

Generally, both of GFRP and BFRP reinforcing bars had the same effect on the one-way concrete slabs. In balance-reinforced one-way concrete slabs, BFRP were more effective, and this is logical because the tensile strength of BFRP is more than GFRP tensile strength. On the other hand, GFRP bars had a better performance on the over-reinforced one-way concrete slabs. That is because the ribbed surface of GFRP reinforcing bars give much more bonding force and with doubling the reinforcement bars the bonding force jumped up and give better results even with a quite weaker material in tensile strength. There was little to no effect for the BMF volume fraction on the type of reinforcement. The behavior of slabs did not change by changing the BMF volume fraction.

4.5.1.3 Effecting of Basalt Macro-Fiber Volume Fraction on Deflection at Mid-Span

One of the main targets of this research is to study the effectiveness of BMF on concrete reinforced with FRP reinforcing bars. Load - deflection relationships of one-way concrete slabs A1, A2 and A3 were shown in Figure 34. Cracking moments were increased with increasing BMF volume fraction. It was increased by 74.18% from A1 to A3 and A2 was in around the middle between them. Also, stiffness was improved with increasing of BMF volume fraction, and the ultimate load was increased by 14.05% from A1 to A3. The ductility was better with increasing BMF volume fraction, and so the failure deflection was increased also from A1 to A3 by 2.9%.

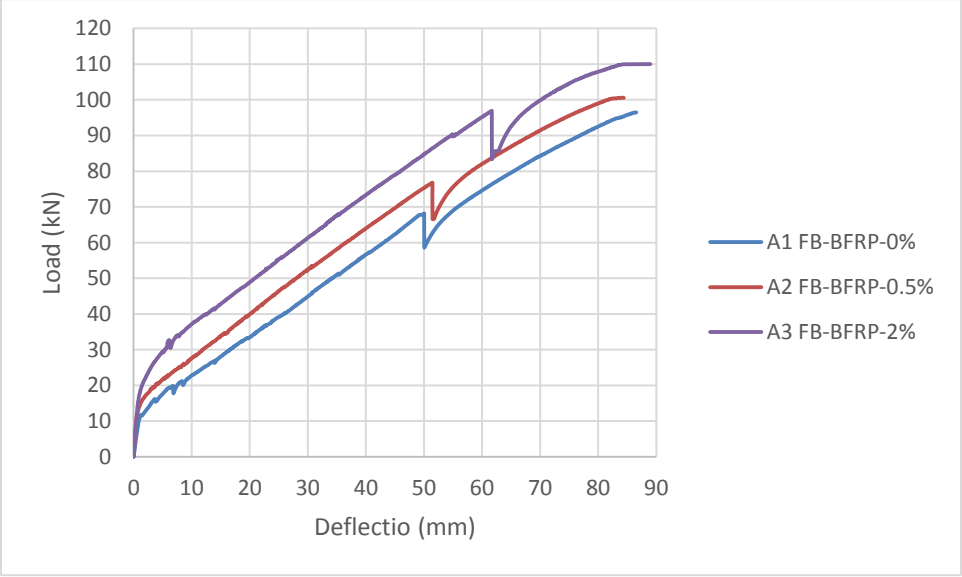

Figure 34. A1, A2 & A3 Load - Deflection Relationships

Figure 35 compares between one-way concrete slabs A4, A5, A6 and A7. Cracking moments were increased by approximately 4 kN between each two of them in a series with increasing BMF volume fraction. A4 and A5 had approximately same stiffness and so A6 and A7. Ultimate loads of A4 and A5 were approximately equal, but A7 was greater by 16.34% than A6. Deflection was increased and ductility was enhanced with increasing BMF volume fraction, and it is good to mention that it was approximately the same for one-way slabs A5 and A6.

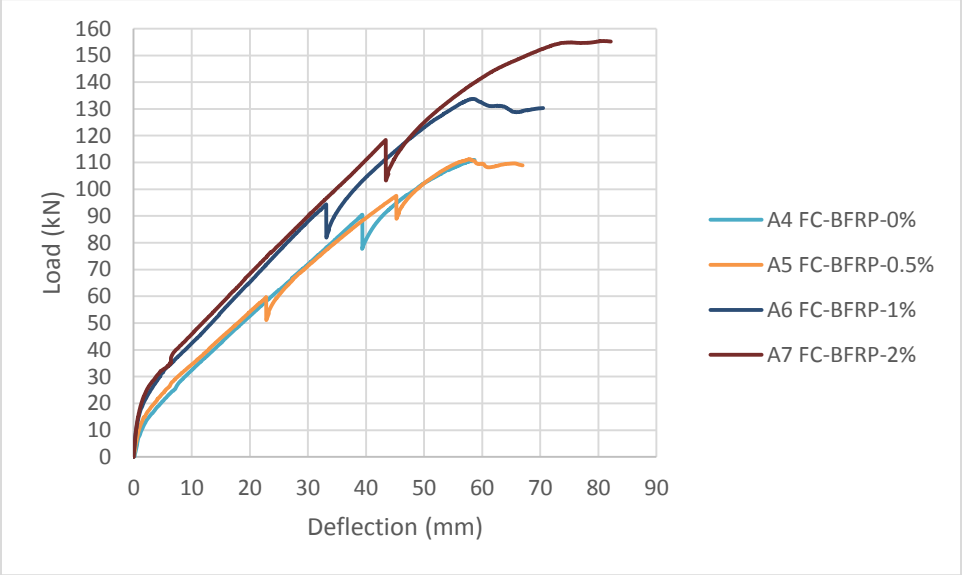

Figure 35. A4, A5, A6 & A7 Load - Deflection Relationships

From Figure 36 shows one-way concrete slabs A8, A9 and A10. Again cracking moments were increased with BMF addition. Stiffness of A9 and A10 were the same and more than the stiffness of A8. Deflection at failure and ultimate load also increased with increasing BMF volume fraction and the behaviors were generally brittle with little more ductility with the presence of BMF.

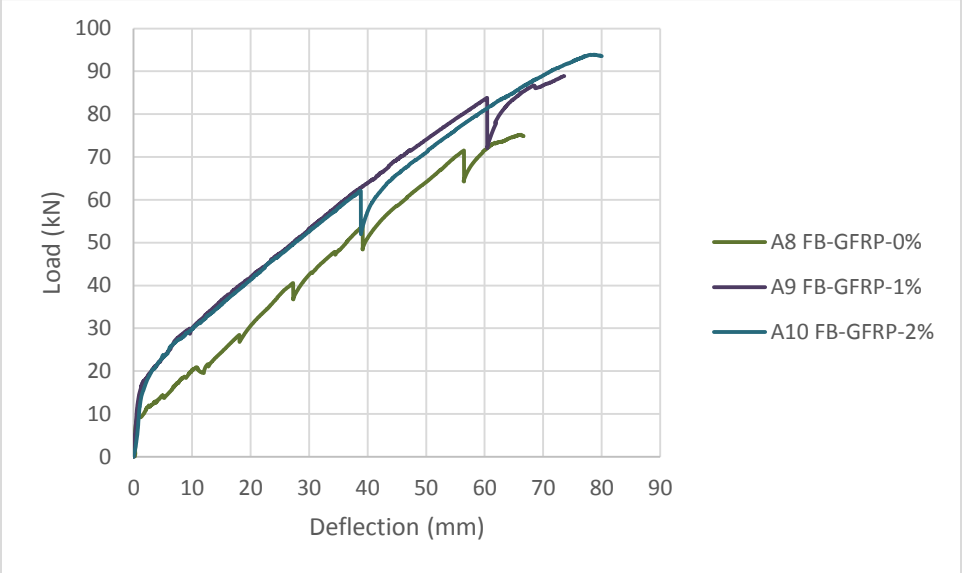

Figure 36. A8, A9 & A10 Load - Deflection Relationships

Figure 37 shows behaviors of slabs A11 and A12. Cracking moments were increased with BMF volume fraction increasing, and also the stiffness, deflections at failure, ultimate loads and ductility.

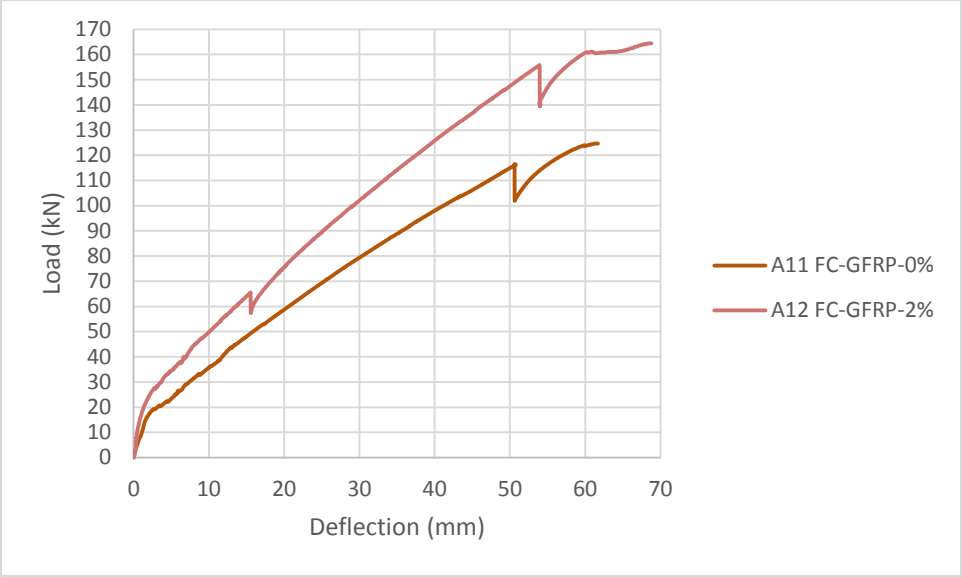

Figure 37. A11 & A12 Load - Deflection Relationships

It can be concluded that the BMF volume fraction had a significant influence on the cracking moment, because it is enhancing the concrete ductility by acting as mini reinforcing bars spreading and distributed in the whole concrete matrix. Ultimate strength also was increased with adding BMF, but the clear difference was between 0% and 2% volume fraction. This because the effect of using 0.5% and 1% of BMF was approximately the same. This is another reason of that the clear effect of BMF on slab ductility appeared in 2% volume fraction in addition to the effect of the over-reinforced ratio as mentioned earlier.

The main control parameter on the one-way concrete slab deflection was the reinforcement ratio, which give a clear difference between samples. But it did not affect

ductility of one-way slabs and the cracking moment. The BMF volume fraction affects mainly after reaching 2% of concrete volume, even its affecting was minor comparing with reinforcement ratio affecting. Type of reinforcement was not affected mainly on one-way slab flexure, but it is better to use ribbed surface FRP reinforcing bars to get better results with increasing reinforcement ratio and there was no effecting of the type of reinforcing bars with respect to changing BMF volume fraction.

4.5.2 Concrete Ductility Index

Concrete ductility is the ability of concrete acting elastically and to increase its deflection without increasing in stresses. It is an important sign in concrete structures while it is acting as a warning for inhabitance to escape before collapsing. SRC structures are designed to fail in tension zone first, because steel reinforcing bars is a ductile material meanwhile concrete is a brittle material. So if the concrete failed before steel reinforcing bars, the structure will collapse suddenly without any warning. One of the main problems of FRP reinforced concrete structures is that both concrete matrix and FRP reinforcing bars are brittle materials. But macro-fibers enhances the ductility of concrete, so that it is very important to calculate the ductility index of FRP reinforced concrete. In SRC ductility index is calculated using values of loads and deflections at yield point, but this method is not appropriate for FRP reinforced concrete because there is no yielding in this type of structures. Many studies developed plenty of methods for calculating ductility index of FRP reinforced concrete, the energy-based approach is one of these methods. According to energy-based approach method, the ductility index is the ratio of the total energy to the elastic energy (Belarbi, 2011), these energies are shown in Figure 38.

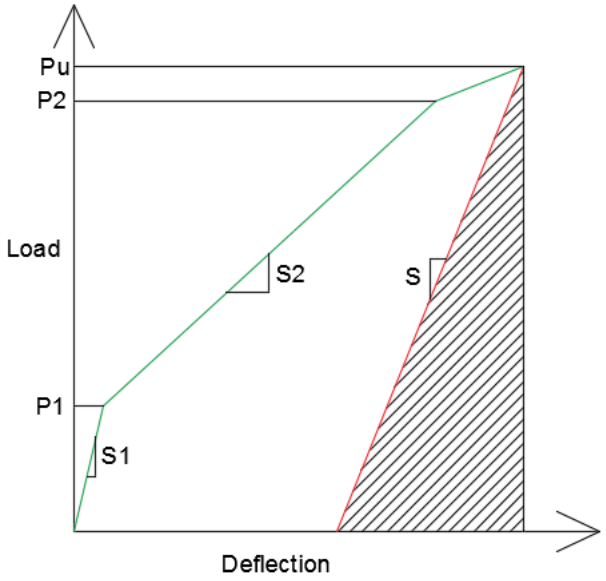

Figure 38. Ductility Index by Energy-Based Approach Method

Where the total absorbed energy is the total area under the load-deflection curve, the elastic absorbed energy is the area hatched in Figure 38, P_1 could be defined as P_{cr} and P_2 could be defined as the load value where the behave of the one-way slab turns to some elasticity. In FRP reinforced concrete elements this value is very close to P_u, the slope S could be calculated using Equation 7.

$$S = \frac{P_1 S_1 + (P_2 - P_1) S_2}{P_2} \qquad \text{Equation 7}$$

The ductility index could be calculated using Equation 8 defined by (Naaman, 1995).

$$\mu_E = 0.5 \left(\frac{E_t}{E_e} + 1 \right) \qquad \text{Equation 8}$$

Where μ_E is the ductility index, E_t is the total absorbed energy and E_e is the elastic absorbed energy.

Table 8 presents ductility index values after calculations. However in order to evaluate the effect of each parameter of three main parameters on the ductility index, individual comparisons for each equivalent samples of each parameter must be studied.

Table 8 Ductility Index Values

Slab	Ductility Index
A1 (FB-BFRP-0%)	1.43
A2 (FB-BFRP-0.5%)	1.89
A3 (FB-BFRP-2%)	2.12
A4 (FC-BFRP-0%)	1.13
A5 (FC-BFRP-0.5%)	1.52
A6 (FC-BFRP-1%)	1.66
A7 (FC-BFRP-2%)	1.78
A8 (FB-GFRP-0%)	1.88
A9 (FB-GFRP-1%)	2.02
A10 (FB-GFRP-2%)	1.8
A11 (FC-GFRP-0%)	1.25
A12 (FC-GFRP-2%)	1.47

4.5.2.1 Effecting of Reinforcement Ratio on Concrete Ductility Index

Figure 39 shows comparisons between equivalent one-way slab samples according to reinforcement ratios, it is clear that in all samples balanced reinforced one-way concrete slab samples were higher in ductility index. That is because in over-reinforced samples FRP reinforcing bars are enhancing the resistance of the one-way concrete slab but in balanced reinforced ratio the concrete mix acting more and affecting more on the general behavior of the one-way concrete slab sample. Also in over-reinforced samples, FRP reinforcing bars are enhancing the resistance of the one-way concrete slab, which increases the load resisted in a linear manner before failure. This increase in load resisted decreases the opportunity of study the ductility index in an ideal way.

Figure 39. Ductility Index Comparisons Due to Reinforcement Ratio

4.5.2.2 Effecting of Reinforcement Type on Concrete Ductility Index

From comparisons were shown in Figure 40, ductility indexes of GFRP reinforced concrete were higher than that in BFRP reinforced concrete in case of balanced reinforced samples. But in over-reinforced samples ductility indexes of BFRP reinforced concrete were higher. This difference happened because in case of balanced reinforced samples BFRP bars are higher in tensile strength than GFRP reinforcing bars, but the ribbed surface of GFRP reinforcing bars resulted in an improvement in their performance by increasing the bonding force between FRP reinforcing bars and surrounding concrete, then the effect of FRP reinforcing bars became more noticeable. This enhancement is clear in case of over-reinforced case, so that in over-reinforced samples the ductility index of GFRP reinforced sample was less than that in BFRP reinforced concrete.

Figure 40. Ductility Index Comparisons Due to Reinforcement Type

4.5.2.3 Effecting of Basalt Macro-Fiber Volume Fraction on Concrete Ductility Index

From results shown in Figure 41, it can be identified that ductility indexes were increased with increasing BMF volume fraction. This increasing is because these fibers are distributed all around the concrete matrix, then acting as mini reinforcing bars trying to

resist cracking of concrete and bond cracked sections together. This performance by BMF allowing concrete to act in a ductile manner before failure.

Figure 41. Ductility Index Comparisons Due to BMF Volume Fraction

4.5.3 Concrete Cracks

Figure 42 shows cracks' locations, lengths and numbers of all one-way concrete slabs samples after failure. In all samples, cracks were concentrated in the mid-span with distances vary between 40 cm and 60 cm between the support and nearest crack. Major cracks started appearing from the bottom about values of the cracking moment in each one-way concrete slab sample and continued in forming and rising toward the top with increasing the load until failure. Cracks did not reach the top of each one-way concrete slab sample, because all of them were failed from top surface compression due to the design for compression control. Most of the cracks were flexural cracks, because one-way concrete slabs were designed to fail due to flexure, not shear forces.

A1

A2

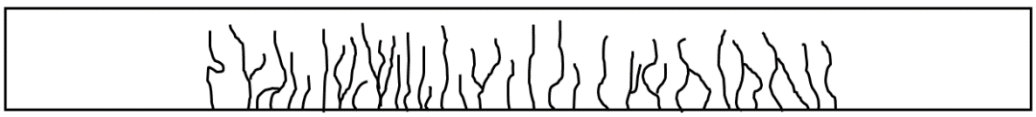

A3

A4

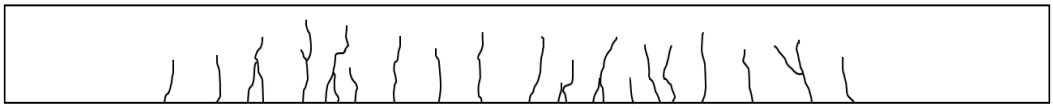

A5

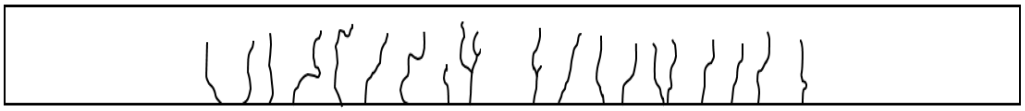

A6

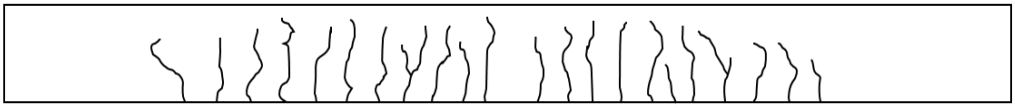

A7

A8

A9

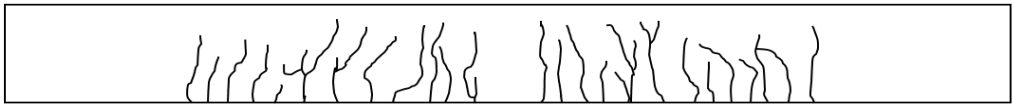

A10

A11

A12

Figure 42. Cracks' Locations, Lengths and Numbers of all One-Way Concrete Slabs

Table 9 presents numbers of cracks in each one-way concrete slab sample. Cracks numbers vary due to differences in three main factors. To study effects of each factor, similar samples should be compared with each other.

Table 9 Cracks' Numbers of all One-Way Concrete Slabs

Slab	Number of Cracks
A1 (FB-BFRP-0%)	15
A2 (FB-BFRP-0.5%)	16
A3 (FB-BFRP-2%)	28
A4 (FC-BFRP-0%)	14
A5 (FC-BFRP-0.5%)	18
A6 (FC-BFRP-1%)	19
A7 (FC-BFRP-2%)	22
A8 (FB-GFRP-0%)	12
A9 (FB-GFRP-1%)	19
A10 (FB-GFRP-2%)	25
A11 (FC-GFRP-0%)	12
A12 (FC-GFRP-2%)	21

4.5.3.1 Effecting of Reinforcement Ratio on Concrete Cracks

Cracks were more in case of balanced reinforced ratio than cracks in case of over-reinforced ratio. The main reason of that is because in over-reinforced one-way slabs, a larger number of FRP reinforcing bars are carrying tensile stresses and that makes less tensile stresses on the concrete matrix, which helps the concrete to uncrack. Also, the shortage in ductility of over-reinforced one-way slabs made reductions in the cracks number.

4.5.3.2 Effecting of Reinforcement Type on Concrete Cracks

In BFRP reinforced one-way slabs cracks were more than cracks of one-way slabs reinforced by GFRP reinforcing, bars. That is because the ribbed surface of GFRP reinforcing bars is working as a concrete holder that denying it from stretch and crack. While the sand coated surface of BFRP reinforcing bars cannot hold the concrete by the same quality.

4.5.3.3 Effecting of Basalt Macro-Fiber Volume Fraction on Concrete Cracks

From Figure 42, it is clear that numbers of cracks were increased with increasing the BMF volume fraction. Because adding BMF is enhancing the ductility of one-way concrete slabs, where one-way concrete slab will deflect more and the probabilities of getting more cracks will be increased. Another reason of increasing cracks with BMF is that BMF is working as stress distributer along the whole one-way concrete slab and that allows the one-way concrete slab to carry the load with more microsections.

4.5.4 FRP Bars Tensile Strain

Table 10 presents values of maximum tensile strains of FRP reinforcing bars. Values were taken from the attached four strain gauges in four different FRP reinforcing bars in one-way concrete slabs tension zones and taking average values from these strain gauges. To get a better understanding and more clear picture of the effect of each factor, on bar tensile strains, samples that same in other factors and different in values of the parameter wanted to be studied will be compared together.

Table 10 Maximum Bars Tensile Strain Values

Slab	Maximum Bar Tensile Strain (μm)
A1 (FB-BFRP-0%)	18527
A2 (FB-BFRP-0.5%)	20258
A3 (FB-BFRP-2%)	21831
A4 (FC-BFRP-0%)	13639
A5 (FC-BFRP-0.5%)	12228
A6 (FC-BFRP-1%)	14166
A7 (FC-BFRP-2%)	16138
A8 (FB-GFRP-0%)	8748*
A9 (FB-GFRP-1%)	10060
A10 (FB-GFRP-2%)	14632
A11 (FC-GFRP-0%)	16671
A12 (FC-GFRP-2%)	8951*

* Strain gauges failed before test end

4.5.4.1 Effecting of Reinforcement Ratio on Bar Tensile Strain

Figure 43 shows effects of reinforcement ratio on the tensile strain of the FRP bars. It can be identified that increasing the reinforcement ratio resulted in a decrease in the bar tensile strain by 35% to 65%. This because stresses are distributed on main elements resisting the tensile force in the bottom of the simply supported one-way concrete slab, which are the reinforcing bars. All FRP reinforcing bars were strained in a brittle manner. This is because of the brittle nature of BFRP and GFRP reinforcing bars. Graphs show that reinforcing bars in both balanced reinforced and in over-reinforced cases started straining

together in the same level because the reinforcement ratio is not a controller factor of cracking moment as discussed in deflection results discussion and this is another evidence of that before cracking concrete matrix is the resisting element of tensile forces.

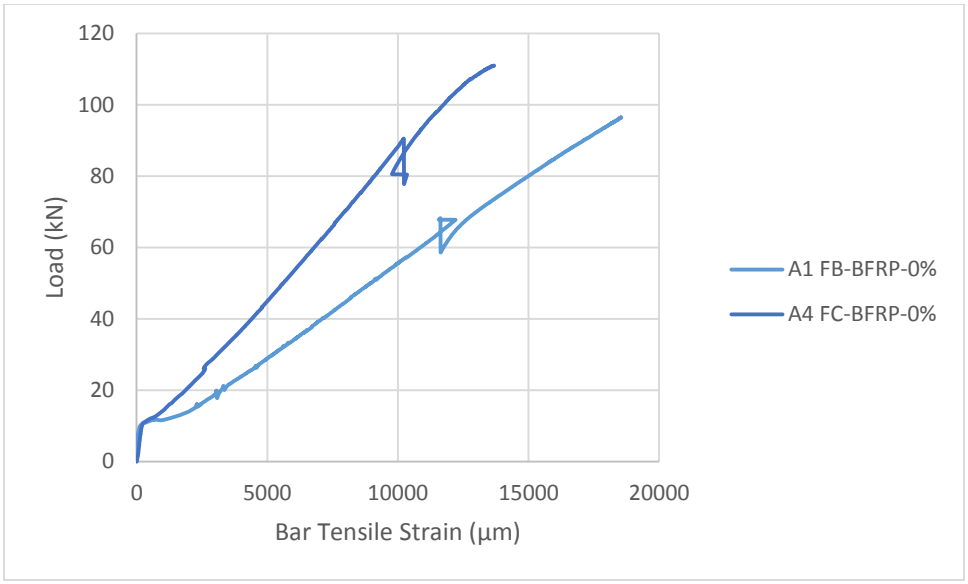

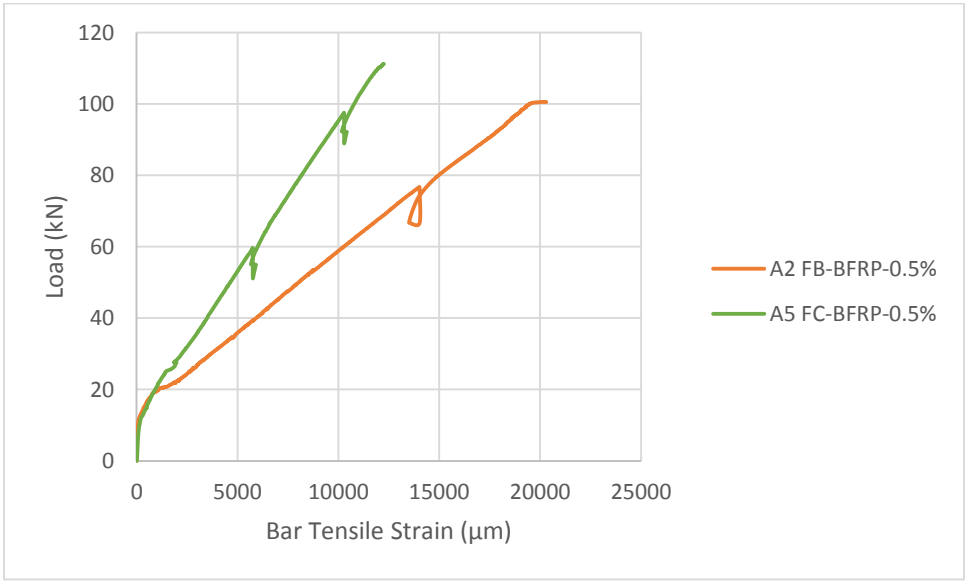

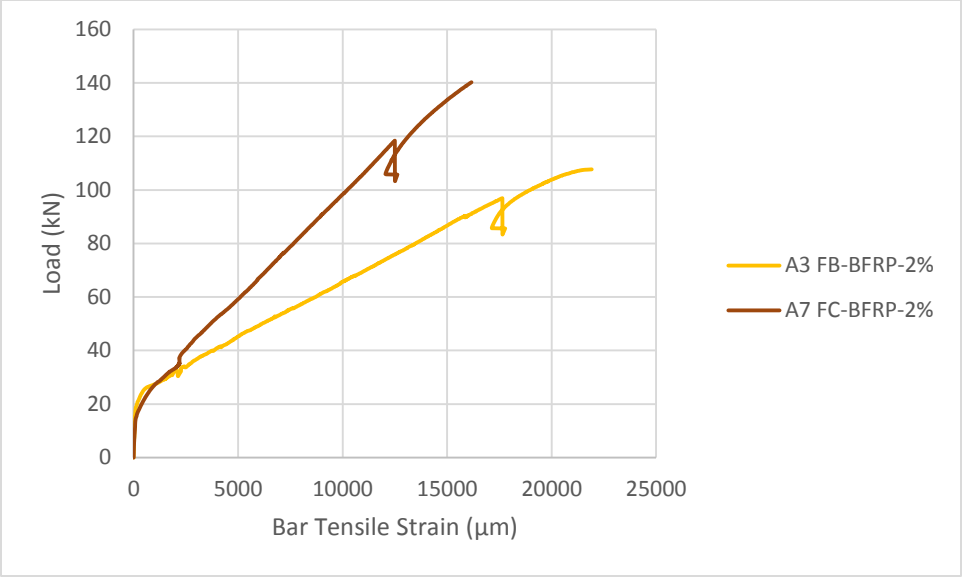

Figure 43. Comparing Load - Bar Tensile Strain Relationships due to Reinforcement Ratio

4.5.4.2 Effecting of Basalt Macro-Fiber Volume Fraction on Bar Tensile Strain

Figure 44 is comparing the behaviors of bar tensile strains with different BMF volume fractions. It is clear that bar tensile strains increased with increasing of BMF volume fraction. The reason of that, is increasing in the concrete ductility by increasing the BMF volume fraction makes the deflection increases. So with the bonding force between the concrete matrix and reinforcing bars, these reinforcing bars strained under tensile force more with increasing of BMF volume fraction.

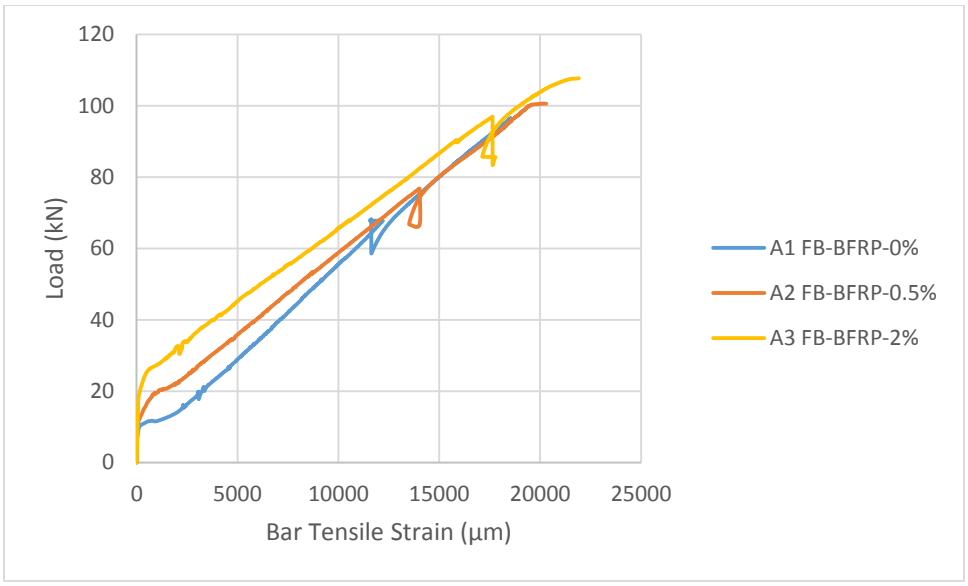
120
100
80
60
40
20
0
Load (kN)
0
5000
10000
15000
20000
25000
Bar Tensile Strain (µm)
A1 FB-BFRP-0%
A2 FB-BFRP-0.5%
A3 FB-BFRP-2%

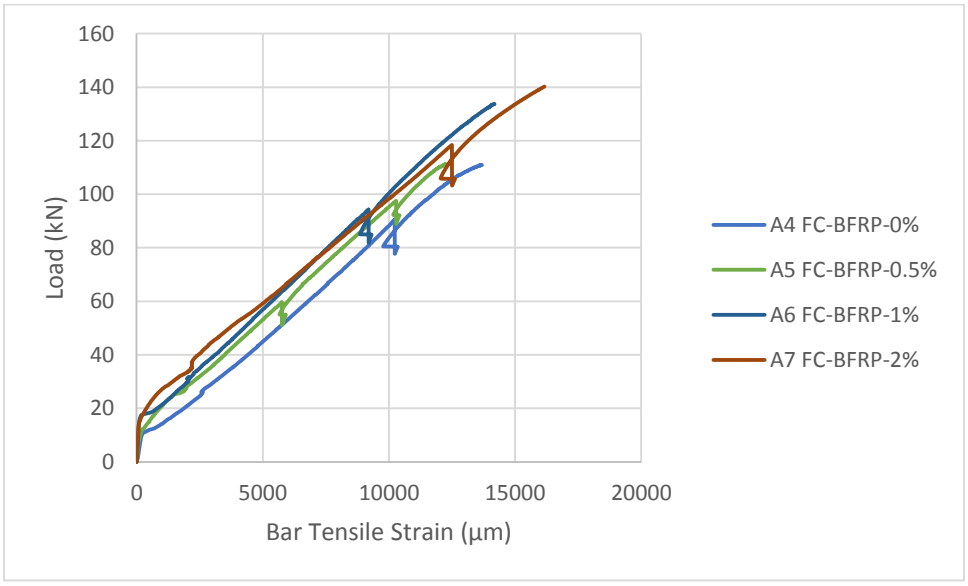
160
140
120
100
80
60
40
20
0
Load (kN)
0
5000
10000
15000
20000
Bar Tensile Strain (µm)
A4 FC-BFRP-0%
A5 FC-BFRP-0.5%
A6 FC-BFRP-1%
A7 FC-BFRP-2%

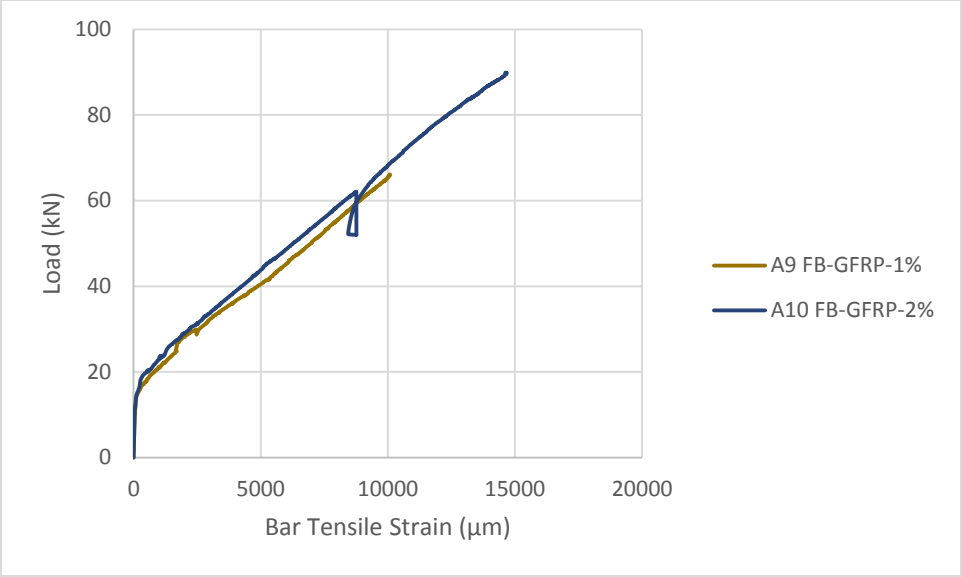

Figure 44. Comparing Load - Bar Tensile Strain Relationships due BMF Volume Fraction

4.5.5 Concrete Compressive Strain

Concrete compressive strains were measured through two concrete strain gauges pasted on the top surface of one-way concrete slab samples, and the average of these two gauges was calculated as mentioned in experimental program chapter. Table 11 shows maximum concrete compressive strain values were taken from test of each one-way concrete slab sample. To differentiate between three main factors affecting, samples that equaled in other factors and different in values of parameter wanted to be studied will be compared together.

Table 11 Maximum Concrete Compressive Strain Values

Slab	Maximum Concrete Compressive Strain (µm)
A1 (FB-BFRP-0%)	3402
A2 (FB-BFRP-0.5%)	3715
A3 (FB-BFRP-2%)	3947
A4 (FC-BFRP-0%)	3330
A5 (FC-BFRP-0.5%)	3660
A6 (FC-BFRP-1%)	3781
A7 (FC-BFRP-2%)	3863
A8 (FB-GFRP-0%)	2380
A9 (FB-GFRP-1%)	2500
A10 (FB-GFRP-2%)	3700
A11 (FC-GFRP-0%)	3254
A12 (FC-GFRP-2%)	3317

4.5.5.1 Effecting of Reinforcement Ratio on Concrete Compressive Strain

Samples with balanced reinforced ratio had larger values of concrete compressive strains than samples with over-reinforced ratio. Same results in deflection and bar tensile strain. This because increasing reinforcement ratio resulted in a decrease in deflection and curvature. So the compressive stress on top service of the concrete sample were less and so the compressive strain in balanced reinforced ratio than over-reinforced ratio.

4.5.5.2 Effecting of Reinforcement Type on Concrete Compressive Strain

From results in Table 11, BFRP reinforced concrete samples had more concrete compressive strains than GFRP reinforced concrete samples. The main reason is due to the surface of FRP reinforcing bars. In case of BFRP reinforcing bars, the sand coated surface does not provide bonding forces between FRP reinforcing bars and surrounding concrete as the ribbed surface of GFRP reinforcing bars. This shortage of bonding force in BFRP reinforced concrete samples allowed concrete to slip from FRP reinforcing bars more and make larger curvatures, then the compressive stress at the top surface of the concrete sample were more and so the concrete compressive strain.

4.5.5.3 Effecting of Basalt Macro-Fiber Volume Fraction on Concrete Compressive Strain

The concrete compressive strain increased with increasing of the BMF volume fraction. This is applicable with increasing of deflection and bar tensile strain with increasing of BMF volume fraction. The reason of that is due to increasing the curvature with increase the deflection.

Results of concrete compressive strain give better understanding especially for the behavior of concrete samples due to the surface of FRP reinforcing bars, and importance of ribbed surface and its advantages on the sand coated surface that it give more stability for the concrete due to increase bonding force between FRP reinforcing bars and surrounding concrete. Increasing reinforcement ratio and decreasing BMF volume fraction made the concrete compressive strain decreased and that was applicable to their effects on deflections and bar tensile strains, and it was expected.

CHAPTER 5: ANALYTICAL PROGRAM

5.1 FLEXURAL CALCULATIONS

5.1.1 Ultimate Moment Prediction

This research is to study combined effects of FRP reinforcing bars and BMF on flexure of one-way concrete slabs. To get the best prediction of ultimate moment both ACI 440 and ACI 544 will be used to come up with theoretical ultimate moment equation. The tension force of FRP reinforcing bars is calculated using Equation 9 (ACI 440.1R, 2008):

$$T_b = \rho_f f_f \left(1 - 0.59 \frac{\rho_f f_f}{f_c}\right) bd \qquad \text{Equation 9}$$

Where T_b is the tension force of FRP reinforcing bars and f_f is the tension stress of FRP reinforcement. It is used because in FRP reinforced concrete, one-way slabs are failed under compression and FRP reinforcing bars do not reach their maximum tensile strength. f_f is calculated by Equation 10 (ACI 440.1R, 2008):

$$f_f = \sqrt{\frac{(E_f \varepsilon_{cu})^2}{4} + \frac{0.85\beta_1 f_c}{\rho_f} E_f \varepsilon_{cu}} - 0.5 E_f \varepsilon_{cu} \qquad \text{Equation 10}$$

ACI 544 estimated effects of BMF on ultimate moments of one-way concrete slabs. The tension force of fibrous concrete is calculated using Equation 11 (ACI 544.4R, 1999):

$$T_{fi} = \sigma_T b(h - e) \qquad \text{Equation 11}$$

Where T_{fi} is the tension force of fibrous concrete, σ_T is the tensile stress in fibrous concrete calculated by Equation 12 and e is the distance from extreme compression fiber to top of the tensile stress block of the fibrous concrete calculated by Equation 13 and showed in Figure 45 (ACI 544.4R, 1999):

$$\sigma_T = 0.00772 V_f F_{be} \frac{l_{fi}}{d_{fi}}$$ Equation 12

$$e = (\varepsilon_{fi} + 0.003)\frac{c}{0.003}$$ Equation 13

Where V_f is the BMF volume fraction, F_{be} is the bond efficiency of the fiber ($F_{be} = 1.1$), l_{fi} is the fiber length, d_{fi} is the fiber diameter (l_{fi} and d_{fi} are from Table 1), ε_{fi} is the fiber tensile strain calculated by Equation 14 and c is the distance from extreme compression fiber to the neutral axis showed in Figure 45 (ACI 544.4R, 1999):

$$\varepsilon_{fi} = \frac{\sigma_{fi}}{E_{fi}}$$ Equation 14

Where σ_{fi} is the fiber stress ($\sigma_{fi} = 2.3\text{MPa}$) (ACI 544.4R, 1999) and E_{fi} is the fiber modulus of elasticity from Table 1.

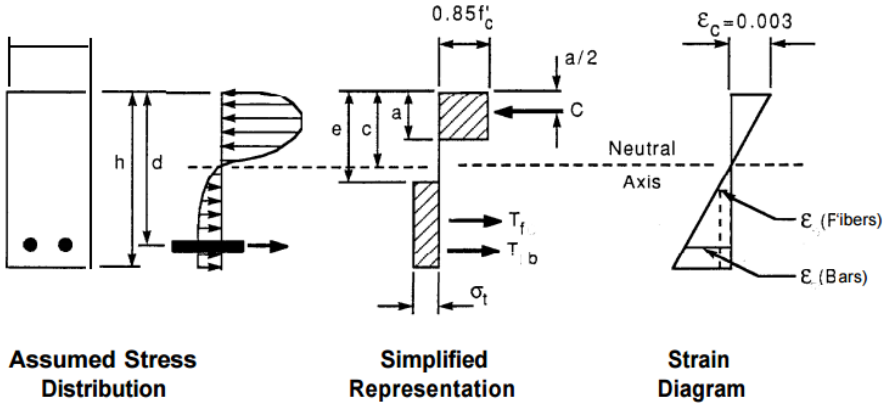

Figure 45. Design Assumptions for Analysis of Singly FRP Reinforced Concrete Beam Containing BMF

After Combining Equations 9 and 11, the theoretical ultimate moment is calculated by Equation 15:

$$M_n = T_b d + T_{fi}\left(\frac{h}{2} + \frac{e}{2}\right) \qquad \text{Equation 15}$$

Values in Table 12 shows that, theoretical ultimate moments are larger than experimental ultimate moments except in over-reinforced one-way slabs with 2% BMF volume fraction. The reduction in the experimental ultimate moment is due to normal losses in quality during mixing and curing. Values are very close to each other, and the accuracy is better than accuracy in cracking moments. In general, the accuracy is less in GFRP reinforced one-way slabs.

Table 12 Experimental and Theoretical Ultimate Moments

Slab	M_u (kN.m)	M_n (kN.m)	M_u / M_a
A1 (FB-BFRP-0%)	38.58	40.15	0.96
A2 (FB-BFRP-0.5%)	40.23	42.22	0.95
A3 (FB-BFRP-2%)	44	48.44	0.91
A4 (FC-BFRP-0%)	44.37	53.39	0.83
A5 (FC-BFRP-0.5%)	44.44	55.44	0.8
A6 (FC-BFRP-1%)	53.36	57.5	0.93
A7 (FC-BFRP-2%)	62.08	61.6	1.01
A8 (FB-GFRP-0%)	29.98	40.15	0.75
A9 (FB-GFRP-1%)	35.53	44.3	0.8
A10 (FB-GFRP-2%)	37.53	48.44	0.77
A11 (FC-GFRP-0%)	49.86	53.39	0.93
A12 (FC-GFRP-2%)	65.76	61.6	1.07

5.2 ANALYTICAL MODELS FOR DEFLECTION CALCULATIONS

5.2.1 Code Base Analytical Design

Currently, codes and guidelines like ACI 440 and CSA S806 provide guidance and equations only for concrete reinforced by glass, aramid and carbon FRP. In this research, a comparison between experimental deflection values with analytical deflection values computed using different codes and guidelines are shown to realize the accuracy of the work done in this research.

The maximum deflection of simply supported one-way slab acted by two points load as shown in Figure 46 is located at the mid-span and calculated using Equation 16.

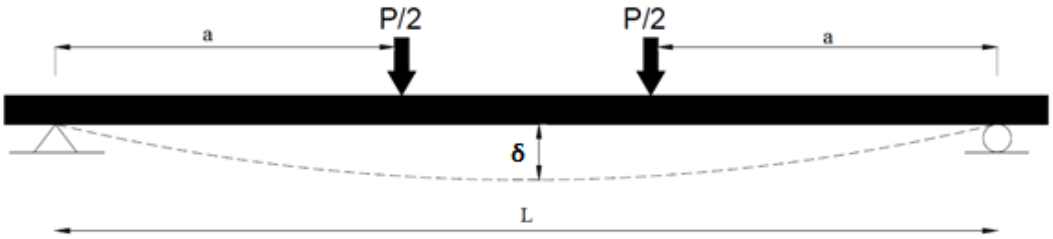

Figure 46. Simply Supported One-Way Slab Acted by Two Points Load

$$\delta_{max} = \frac{Pa}{48E_c I_e}(3L^2 - 4a^2) \qquad \text{Equation 16}$$

Where δ_{max} is the maximum deflection, P is the total load applied by the universal test machine, a is the distance between the support and the nearest point load, L is the span length, E_c is the modulus of elasticity of concrete calculated by Equation 17 and I_e is the effective moment of inertia.

$$E_c = 4700\sqrt{f'_c} \qquad \text{Equation 17}$$

The effective moment of inertia is calculated according to the code or guideline used. Regarding (ACI 440-15) the effective moment of inertia is calculated by Equation 18:

$$I_e = \frac{I_{cr}}{1-\gamma\left(\frac{M_{cr}}{M_a}\right)^2\left(1-\frac{I_{cr}}{I_g}\right)} \leq I_g \qquad \text{Equation 18}$$

Where M_a is the service moment at the critical cross-section of the one-way slab calculated by Equation 19, γ is a factor calculated by Equation 20, I_{cr} is the cracking moment of inertia calculated by Equation 21 and M_{cr} is the cracking moment calculated by Equation 22.

$$M_a = \frac{Pa}{2} \qquad \text{Equation 19}$$

$$\gamma = 1.72 - 0.72\left(\frac{M_{cr}}{M_a}\right) \qquad \text{Equation 20}$$

$$I_{cr} = \frac{bd^3}{3}k^3 + n_f A_f d^2(1-k)^2 \qquad \text{Equation 21}$$

$$M_{cr} = \frac{f_r I_g}{y_t} \qquad \text{Equation 22}$$

Where k is the ratio of the depth of the neutral axis to the reinforcement depth calculated by Equation 23, n_f is the ratio of the modulus of elasticity of FRP reinforcing bars to the

modulus of elasticity of concrete calculated by Equation 24, f_r is the modulus of rupture of concrete calculated by Equation 25 and y_t is the distance from centroidal axis of gross section to tension face.

$$k = \sqrt{2\rho_f n_f + (\rho_f n_f)^2} - \rho_f n_f \qquad \text{Equation 23}$$

$$n_f = \frac{E_f}{E_c} \qquad \text{Equation 24}$$

$$f_r = 0.62\lambda\sqrt{f'_c} \qquad \text{Equation 25}$$

Where λ is a modification factor to reflect the reduced mechanical properties of light weight concrete relative to normal weight concrete of the same compressive strength equals 1 for normal weight concrete.

Equation 21 calculates the cracking moment of inertia only without macro-fibers, (Tan, 1994) rectified this equation by adding parameters as in Equation 26.

$$I_{cr} = \frac{bd^3}{3}k^3 + n_f A_f d^2(1-k)^2 + n_f A_{tf}\frac{(h-c)^2}{3} + (n_f - 1)A_{cf}\frac{c^3}{3} \qquad \text{Equation 26}$$

Where A_{tf} is the area of BMF in tensile zone calculated by Equation 27 and A_{cf} is the area of BMF in compression zone calculated by Equation 28:

$$A_{tf} = \eta_l \eta'_0 V_f b(h-c) \qquad \text{Equation 27}$$

$$A_{cf} = \eta_l \eta_0 V_f bc \qquad \text{Equation 28}$$

Where η_l is the length efficiency factor and it equals 0.5 according to (Lim, 1987), η_0 is the orientation factor before cracking calculated by Equation 29 (Lee, 2010) and η'_0 is the orientation factor after cracking calculated as 0.45 of the orientation factor before cracking

due to the reduction of the effective moment of inertia after cracking is around 0.45 of the gross moment of inertia.

$$\eta_0 = \frac{\int_0^{\pi/2} \frac{I_{fi}}{2} \cos\theta \, d\theta}{\int_0^{\pi/2} \frac{I_{fi}}{2} \, d\theta} \qquad \text{Equation 29}$$

According to (Faza, 1992) the average moment of inertia was proposed by developing Equation 30 to use it instead of the effective moment of inertia in Equation 18:

$$I_m = \frac{23 I_{cr} I_e}{8 I_{cr} + 15 I_e} \leq I_g \qquad \text{Equation 30}$$

Where I_m is the average moment of inertia.

Equation 20 was developed then by Bischoff and Gross to come up with the Equation 31 (Bischoff, 2011):

$$\gamma = \frac{3\frac{a}{L} - 4\left(4\left(\frac{M_{cr}}{M_a}\right) - 3\right)\left(\frac{a}{L}\right)^3}{3\frac{a}{L} - 4\left(\frac{a}{L}\right)^3} \qquad \text{Equation 31}$$

ISIS code developed Equation 32 to calculate the effective moment of inertia (ISIS, 2007):

$$I_e = \frac{I_{cr} I_g}{I_{cr} + \left(1 - 0.5\left(\frac{M_{cr}}{M_a}\right)^2\right)(I_g - I_{cr})} \leq I_g \qquad \text{Equation 32}$$

CSA S806 code developed Equation 33 to calculate the maximum deflection without calculating the effective moment of inertia (CSA S806-02, 2007):

$$\delta_{max} = \frac{PL^3}{48 E_c I_{cr}} \left[3\left(\frac{a}{L}\right) - 4\left(\frac{a}{L}\right)^3 - 8\eta\left(\frac{L_g}{L}\right)^3\right] \qquad \text{Equation 33}$$

Where η is a factor calculated by Equation 34 and L_g is the distance from the support to where service moment equals cracking moment.

$$\eta = 1 - \frac{I_{cr}}{I_g} \qquad \text{Equation 34}$$

Euro Code II developed Equation 35 to calculate the maximum deflection depending on an average value between deflection of the fully cracked section and deflection of the gross section (Eurocode 2, 2004):

$$\delta_{max} = \left(1 - \left(\frac{M_{cr}}{M_a}\right)^2\right)\delta_{cr} + \left(1 - \left(1 - \left(\frac{M_{cr}}{M_a}\right)^2\right)\right)\delta_g \qquad \text{Equation 35}$$

Where δ_{cr} is the deflection of the cracked section and δ_g is the deflection of the gross section.

5.2.2 Comparison between Analytical and Experimental Results

After calculating deflection values using previous methods, for each sample, a graph of each deflection values method has been set and compared with the graph of experimental results of deflection. As shown in Figures 47 – 58, the general behavior of all equations was ductile. In early ages, Faza and CSA equations give far away results from experimental and other equations and their slopes did not change until the maximum load. Other equations cracking points were more than experimental cracking points, especially with low BMF volume fraction. Experimental deflections at failure points where larger than equations with increasing BMF volume fraction.

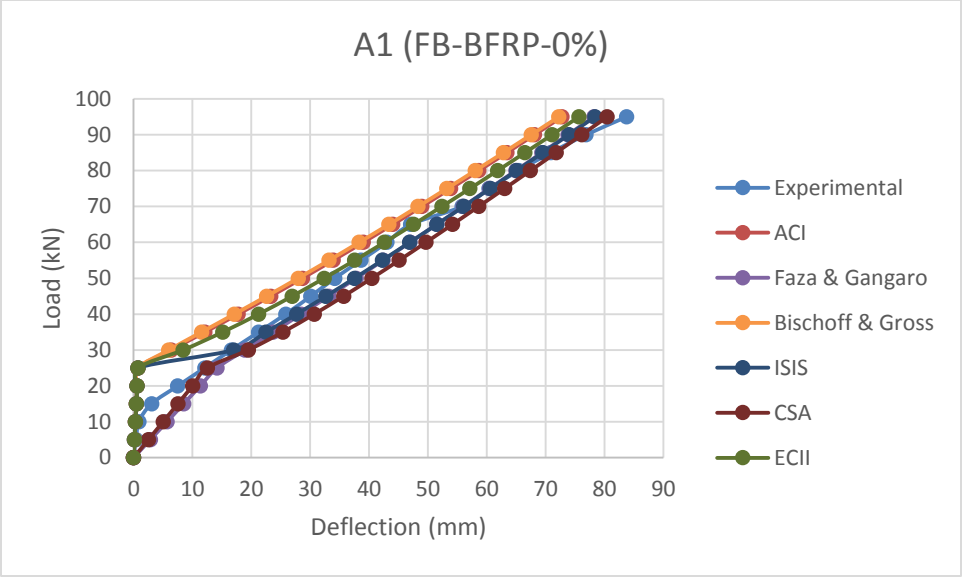

Figure 47. Experimental & Theoretical Deflection Values of A1

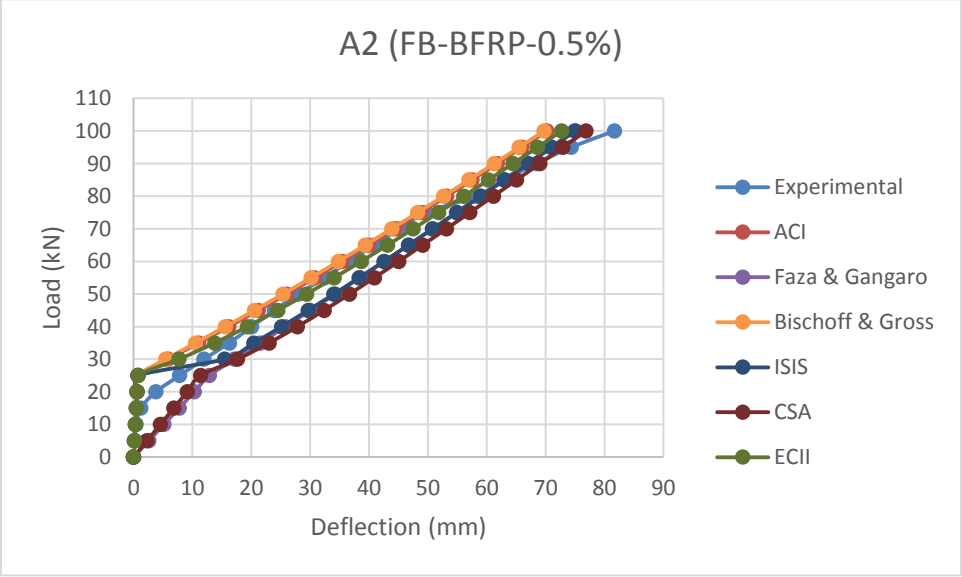

Figure 48. Experimental & Theoretical Deflection Values of A2

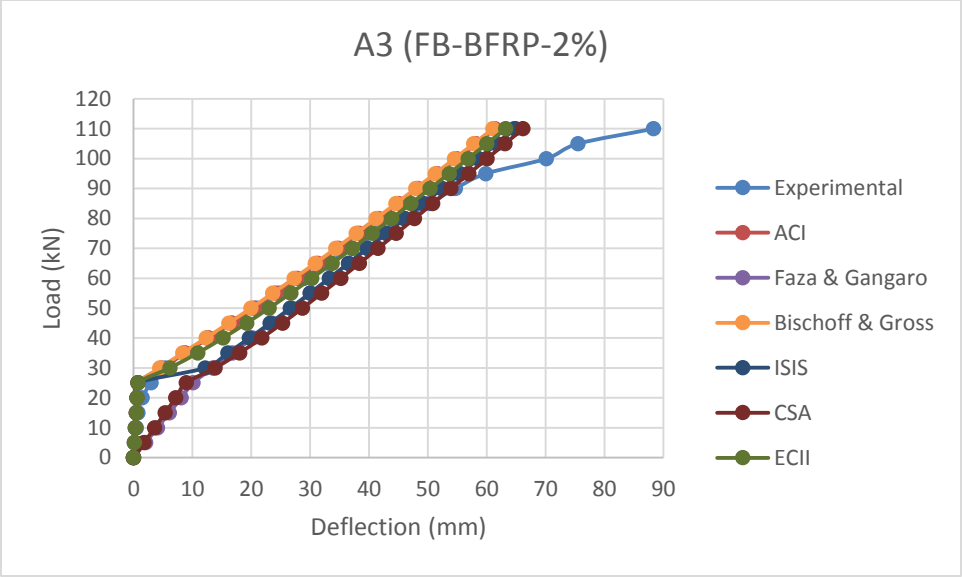

Figure 49. Experimental & Theoretical Deflection Values of A3

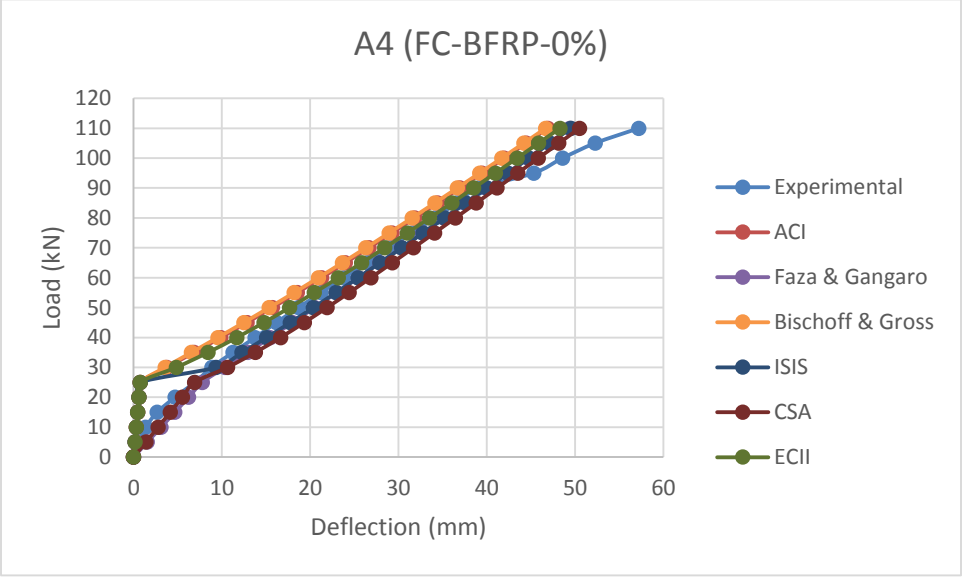

Figure 50. Experimental & Theoretical Deflection Values of A4

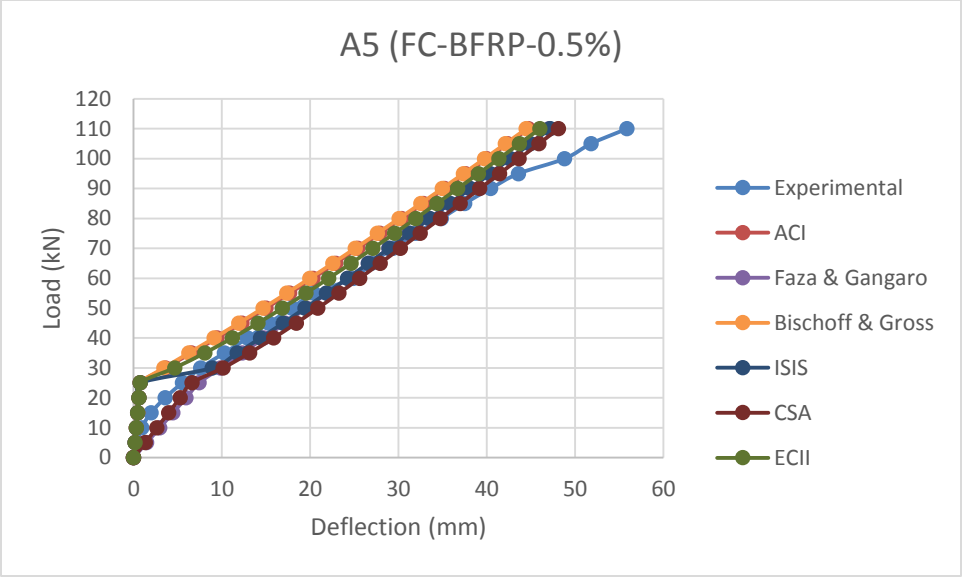

Figure 51. Experimental & Theoretical Deflection Values of A5

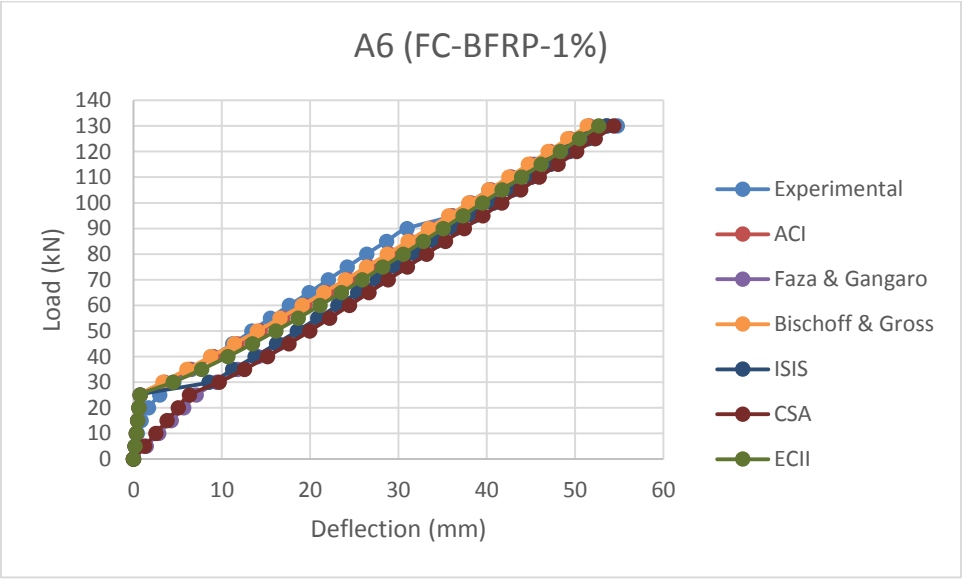

Figure 52. Experimental & Theoretical Deflection Values of A6

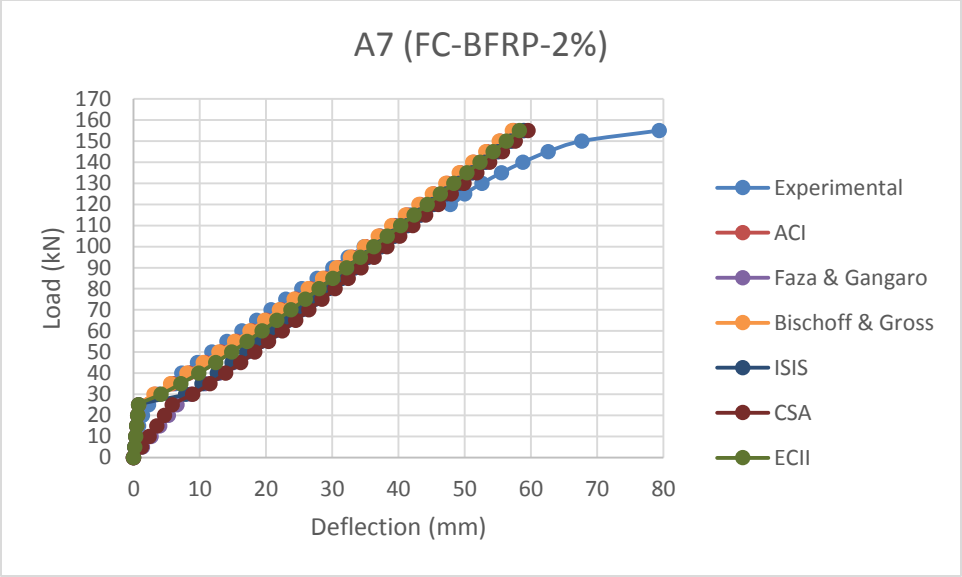

Figure 53. Experimental & Theoretical Deflection Values of A7

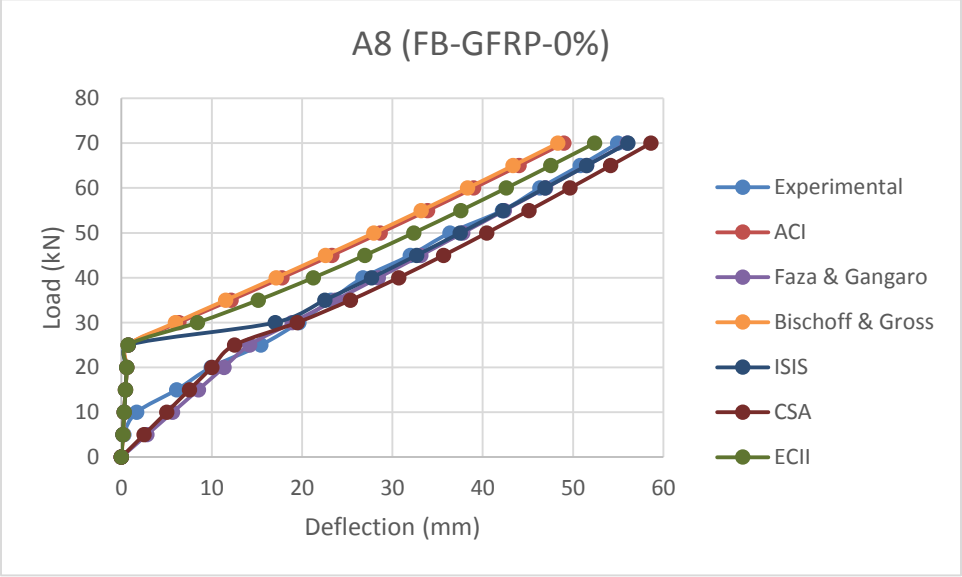

Figure 54. Experimental & Theoretical Deflection Values of A8

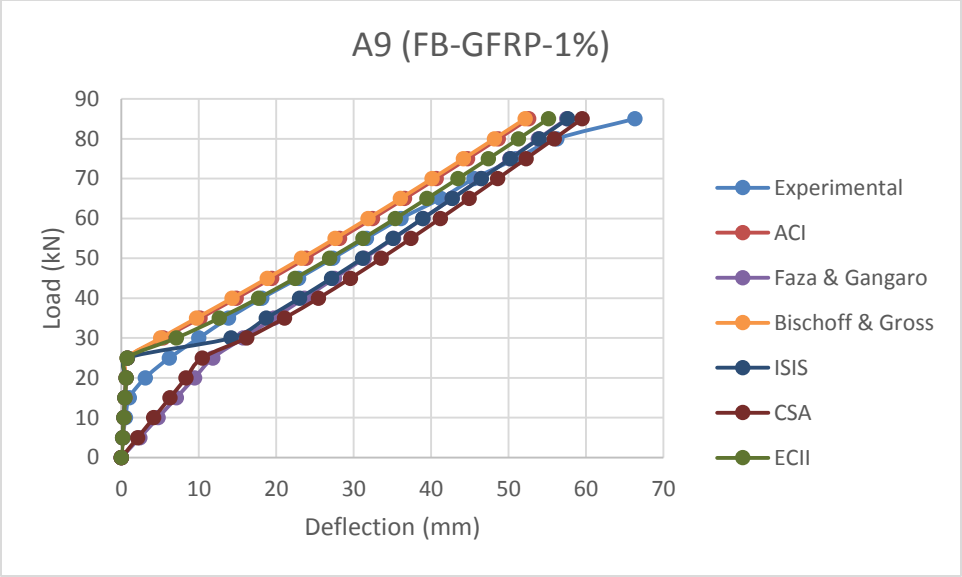

Figure 55. Experimental & Theoretical Deflection Values of A9

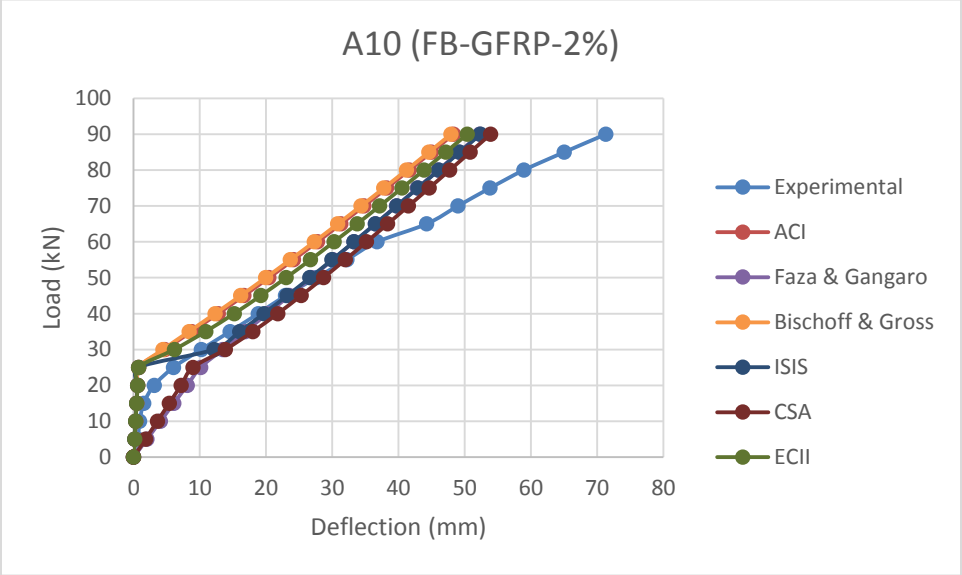

Figure 56. Experimental & Theoretical Deflection Values of A10

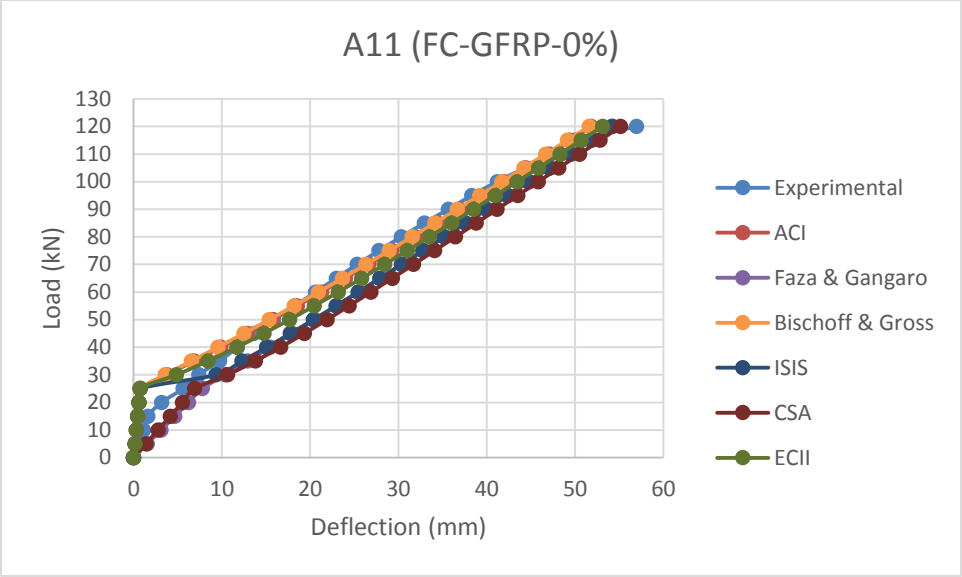

Figure 57. Experimental & Theoretical Deflection Values of A11

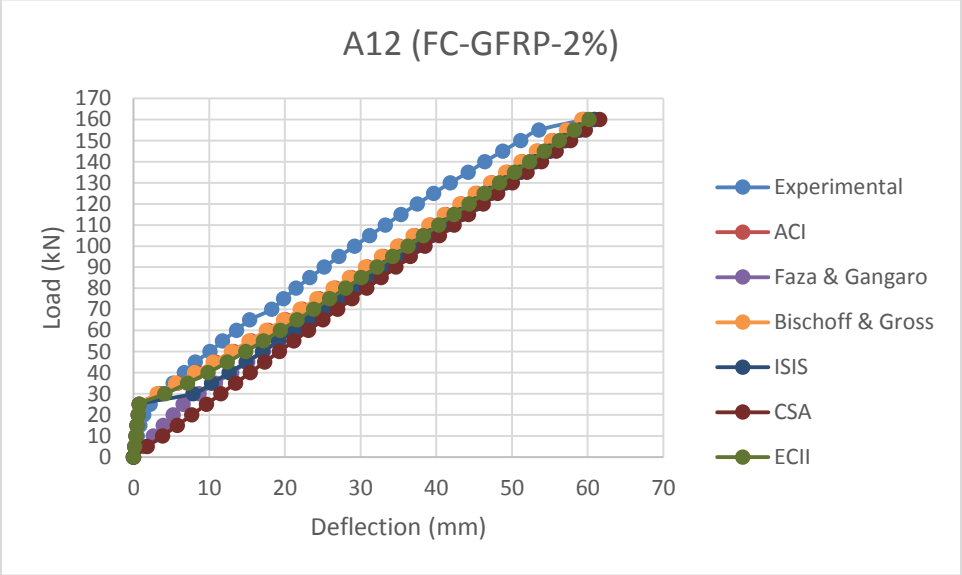

Figure 58. Experimental & Theoretical Deflection Values of A12

CHAPTER 6: SUMMARY, CONCLUSIONS AND RECOMMENDATIONS

6.1 SUMMARY

In this study, the flexural performance and ultimate capacity of FRC one-way concrete slabs reinforced with BFRP reinforcing bars were investigated experimentally and analytically. A total of 12 concrete one-way concrete slab specimens were flexural tested until failure. The parameters investigated included the type of reinforcement (Basalt FRP bars, and Glass FRP bars), reinforcement ratio (1.4 ρ_b, and 2.8 ρ_b), and the BMF volume fraction (0%, 0.5%, 1% and 2%). The deflection, compressive concrete strain at mid-span of the one-way slab were measured and recorded. The testing results were compared with control specimens reinforced by GFRP reinforcing bars and with no added BMF. The testing results of the specimens were compared to the analytical equation for deflection's prediction. Experimental and numerical results showed a general improvement in the flexural behavior of concrete one-way slabs by adding more BMF and increasing the reinforcement ratio. On the other hand, there were no major differences between BFRP and GFRP reinforcing bars. The main difference between them was because of the surface of FRP reinforcing bars. The ribbed surface of GFRP reinforcing bars gives better flexure for concrete one-way slabs than the sand coated surface of BFRP reinforcing bars, especially in over-reinforced samples. Test results clearly showed that both FRP reinforcing bars and BMF can be used as alternative materials for steel reinforcement in concrete structures.

6.2 CONCLUSION

The following conclusion can be drawn based on the finding of the experimental and analytical investigation:

1. There is no relationship between BMF volume fraction and concrete compressive strength. This clearly deduced while adding BMF does not affect the concrete compressive strength.

2. Adding BMF into the concrete mix make great enhancing on concrete tensile strength. This because BMF is working as minibars spread and distributed in the whole concrete mix and provide an immediate tensile load carrying capacity when micro-cracks develop in concrete.
3. The reinforcement ratio has no effects on the cracking moment because before first cracking the only resisting element is the concrete mix.
4. Increasing the reinforcement ratio increases the concrete one-way slabs capacity with decreasing its failure deflection. As a result, the ductility index and cracks number were decreased with increasing the reinforcement ratio because of the brittle nature of FRP reinforcing bars.
5. Tensile bar strain was decreased with increasing reinforcement ratio, because increasing the number of reinforcing bars distributes stresses on more numbers of reinforcing bars and that enhancing their resting.
6. Increasing reinforcement ratio is enhancing the capacity and strength of FRP reinforcing concrete.
7. Cracking moment in FRC is larger than cracking moment of concrete without fibers. This is attributed to the ability of BMF to act as mini reinforcing bars and enhancing concrete tensile strength.

8. Concrete one-way slabs with BMF had more deflection than concrete one-way slabs without BMF. This because the ductility index was increased with increasing

BMF, so the ability of the concrete one-way slab to deflect more under its maximum capacity before failure.

9. Both the concrete ultimate compressive strain and ultimate tensile strain of reinforcing bars were increased with the addition of the volume fraction of BMF.
10. Analytical equations where close to experimental deflection results in general. But these equations does not give ductile manner as BMF gives in experiment.

6.3 RECOMMENDATIONS

Results of this research showed it is recommended to use BMF to enhance the ductility of one-way concrete slabs reinforced with FRP bars. The benefits of BMF may help structural members to function after cracks. FRP and BMF can be an ideal alternative to the traditional SRC in order to enhance the concrete durability. This study will inspire the acceptance of using FRP reinforcing bars in FRC.

REFERENCES

1) ACI 440-15. Guide for Design and Construction of Structural Concrete Reinforced with FRP Reinforcing Bars. ACI Committee 318, American Concrete Institute, Farmington Hills, MI, USA, 2015.
2) ASTM C39/C39M-12a, Standard Test Method for Compressive Strength of Cylindrical Concrete Specimens, ASTM International, West Conshohocken, PA, USA, 2012.
3) Cory High, Hatem M. Seliem, Adel El-Safty and Sami H. Rizkalla (2015). Use of basalt fibers for concrete structures. Construction and Building Materials 96 (2015) 37–46.
4) Jianxun Ma, Xuemei Qiu, Litao Cheng, Yunlong Wang, Experimental research on the fundamental mechanical properties of presoaked basalt fiber concrete, in: Lieping Ye, Peng Feng, Qingrui Yue (Eds.), Advances in FRP Composites in Civil Engineering, Springer, Berlin, Heidelberg, 2011, pp. 85–88.
5) Tumadhir M. Borhan, Thermal and mechanical properties of basalt fibre reinforced concrete, Proc. World Acad. Sci., Eng. Technol. 76 (2013) 313.
6) Berozashvili M. Continuous reinforcing fibers are being offered for construction, civil engineering and other composites applications. Adv. Mater Com. News, Compos Worldwide (2001) 21(6):5–6.
7) Tehmina Ayub, Nasir Shafiq, and M. Fadhil Nuruddin. Effect of Chopped Basalt Fibers on the Mechanical Properties and Microstructure of High Performance Fiber Reinforced Concrete. Hindawi Publishing Corporation, Advances in Materials Science and Engineering, Volume 2014, Article ID 587686, 14 pages.

8) S. U. Khan, M. F. Nuruddin, T. Ayub, and N. Shafiq, “Effects of different mineral admixtures on the properties of fresh concrete,” The Scientific World Journal, vol. 2014, Article ID 986567, 11 pages, 2014.

9) T. Ayub, S. U. Khan, and F. A. Memon, “Mechanical characteristics of hardened concrete with different mineral admixtures: a review,” The Scientific World Journal, vol. 2014, Article ID 875082, 15 pages, 2014.

10) T. Ayub, N. Shafiq, S. Khan, and M. Nuruddin, “Durability of concrete with different mineral admixtures: a review,” International Journal of Civil, Architectural Science and Engineering, vol. 7, no. 8, pp. 199–210, 2013.

11) V. Ramakrishnan, N. S. Tolmare, and V. Brik, Performance Evaluation of 3-D Basalt Fiber Reinforced Concrete & Basalt Rod Reinforced Concrete, 1998.

12) K. Van de Velde, P. Kiekens, and L. van Langenhove, “Basalt fibres as reinforcement for composites,” in Proceedings of 10th International Conference on Composites/Nano Engineering, pp. 20–26,University ofNewOrleans,NewOrleans, Lo,USA, 2003.

13) Patnaik, A.K., Puli, R.K., and Mylavarapu, R., “Basalt FRP: A new FRP material for infrastructure market ?“, 4th International Conference on Advanced Composite Materials in Bridges and Structures (ACMBS-IV) - Editors: M. El-Badry and L. Dunaszegi, Canadian Society of Civil Engineers, Montreal, Canada, July 2004, 8 pages.

14) Patnaik, A., “Applications of Basalt Fiber Reinforced Polymer (BFRP) Reinforcement for Transportation Infrastructure”, Developing a Research Agenda

for Transportation Infrastructure Preservation and Renewal, Transportation Research Board Conference (TRB-2009), Washington, D.C., Nov. 2009, 5 pages.

15) Patnaik, A., Adhikari, S., Bani-Bayat, P., and Robinson, P.,"Flexural Performance of Concrete Beams Reinforced with Basalt FRP Bars", 3rd fib International Congress, Washington, D.C., May 2010, 12 pages.
16) Patnaik, A.,"Basalt Fiber Reinforced Polymer (BFRP) Materials for Reinforced Concrete Applications", 2011 DoD Corrosion Conference, NACE International, Palm Springs, CA July-Aug. 2011, 15 pages.
17) Kim GS, Sim J. Premature failure behavior of RC beams strengthened by plates. J Korean Soc Civil Eng 1999;19(I/4): 561–70.
18) ACI Committee 440, ACI 440.1R-06 – Guide for the Design and Construction of Externally Bonded FRP Systems, (2006).
19) ISIS Canada, Reinforcing Concrete Structures with Fiber Reinforced Polymers. Design Manual N8 3 Version 2, Canada ISIS Canada Corporation, Manitoba, 2007.
20) CSA, S806-12: Design and Construction of Building Components with Fiber-Reinforced Polymers, Canadian Standards Association, Canada, 2012.
21) Japan Society of Civil Engineers (1997). Recommendation for design and construction of concrete structures using continuous fiber reinforcing materials. Concrete Engineering Series 23; Tokyo, Japan Society of Civil Engineers.
22) Benmokrane, B., Wang, P., Ton-That, T. M., Rahman, H., and Robert, J. F. (2002). "Durability of glass fiber-reinforced polymer reinforcing bars in concrete environment." J. Compos. Constr., 10.1061/(ASCE)1090-0268(2002)6:3(143), 143–153.

23) Kameny Vek. (2010). “Advanced basalt fiber.” (http://www.basfiber.com).

24) Yilmaz S, Ozkan OT, Gunay V. Crystallization kinetics of basalt glass. Ceram Int. (1996) 22:477–81.

25) Wei, B., Cao, H., and Song, S. (2010). Environmental resistance and mechanical performance of basalt and glass fibers. Materials Science and Engineering; 527(18-19); 4708-4715.

26) Fahmy, M., Wu, Z., and Wu, G. (2009). “Seismic performance assessment of damage-controlled FRP-Retrofitted RC bridge columns using residual deformations.” J. Compos. Constr., 10.1061/(ASCE)CC.1943-5614.0000046, 498–513.

27) Erlendsson, J. O. (2012). “Continuous basalt fiber as reinforcement material in polyester resin.” M.S. thesis, School of Science and Engineering at Reykjavík Univ., Reykjavík, Iceland.

28) Sim, J., Park, C., and Moon, D. J. (2005). “Characteristic of basalt fiber as a strengthening material for concrete structures.” Compos. Part B, 36(6), 504–512.

29) Lee YT, Lee JH, Hwang HS, Kim YD. Performance of concrete structures retrofitted with fiber reinforce polymers. Mag. Korean Conc. Ins. (2002) 14(4):89–96.

30) Li, H., Xian, G., Ma, M., and Wu, J. (2012). “Durability and fatigue performances of basalt fiber/epoxy reinforcing bars.” Proc., 6th Int. Conf. on FRP Composites in Civil Engineering (CICE 2012), Univ. of Rome La Sapienza, Rome.

31) Ahmed El Refai (2013). Durability and Fatigue of Basalt Fiber-Reinforced Polymer Bars Gripped with Steel Wedge Anchors. J. Compos. Constr. Vol. 17-issue: 6.

32) Andreea Serbescu, Maurizio Guadagnini and Kypros Pilakoutas. Mechanical Characterization of Basalt FRP Rebars and Long-Term Strength Predictive Model. 2014.

33) Xianqi, H., Yifeng, L. and Tunian, S. Basalt Continuous Fiber and its Reinforcing Composite Material [J]. Hi-Tech Fiber & Application, (2002) 27(2):1–6.

34) Wang Mingchao, Zhang Zuoguang, Li Yubin, Li Min and Sun Zhijie. Chemical Durability and Mechanical Properties of Alkali-proof Basalt Fiber and its Reinforced Epoxy Composites. Journal of Reinforced Plastics and Composites (2008) 27: 393.

35) XIAN, G.J., KARBHARI, V.M. DMTA based investigation of hygrothermal ageing of an epoxy system used in rehabilitation. Journal of Applied Polymer Science. Vol. 104, No. 2, (2007), pp. 1084-1094.

36) Marek U., Andrzej L., Andrzej G.(2013). "Investigation on Concrete Beams Reinforced with Basalt Rebar." Procedia Engineering 57 (2013) 1183 – 1191.

37) Jun-Mo Yang, Kyung-Hwan Min, Hyun-Oh Shin, Young-Soo Yoon. (2012). Effect of steel and synthetic fibers on flexural behavior of high-strength concrete beams reinforced with FRP bars, Composites Part B: Engineering, Volume 43, Issue 3, 1077-1086.

38) ACI Committee 544, 1999. State of the Art Report on Fiber Reinforced Concrete Reported (ACI 544.4R-88 Reapproved 1999). ACI Structural Journal, 99(Reapproved).

39) Holschemacher, K., Mueller, T., Ribakov, Y. (2010). Effect of steel fibers on mechanical properties of high-strength concrete. Materials and Design; 31(5); 2604-2615.

40) Mohammadi, Y., Carkon-Azad, R., Singh, S.P., Kaushik, S. (2009). Impact resistance of steel fibrous concrete containing fibers of mixed aspect ratio. Construction and Building Materials; 23(1), 183-189.

41) Katzer, J., Domski, J. (2012). Quality and mechanical properties of engineered steel fibers used as reinforcement for concrete. Construction and Building Materials; 34; 243-248.

42) Sudeep Adhikari (2013). Mechanical and structural characterization of MiniBar reinforced concrete beams. Ph. D. Dissertation.

43) Patnaik A, Banibayat P, Adhikari S, Robinson P. (2012). Mechanical Properties of Basalt Fiber Reinforced Polymer Bars Manufactured Using a Wet Layup Method. International Review of Civil Engineering, Vol. 3, pp 4412-416.

44) Iyer, P., Kenno, S., and Das, S. (2015). "Mechanical Properties of Fiber-Reinforced Concrete Made with Basalt Filament Fibers." 2016 J. Mater. Civ. Eng., 10.1061/(ASCE)MT.1943-5533.0001272, 04015015).

45) Anil K. Patnaik, Len Miller and Per Cato Standal. FIBER REINFORCED CONCRETE MADE FROM BASALT FRP MINIBAR. 2014.

46) Johann Helgi Oskarsson. The Effect of Fibres on the Compressive Ductility of Lightweight Aggregate Concrete. Norwegian University of Science and Technology, Master Thesis 2013.

47) Wang H, Belarbi A. (2005). Flexural Behavior of Fiber-Reinforced-Concrete Beams Reinforced with FRP Rebars.

48) Reddy K. (2015). Flexural Behavior of Steel Fiber Reinforced High Strength Concrete Beams.

49) Chaohua Jiang, Ke Fan, Fei Wu and Da Chen. Experimental study on the mechanical properties and microstructure of chopped basalt fibre reinforced concrete. Materials and Design 58 (2014) 187–193.

50) Ilker Fatih Kara, Ashraf F. Ashour and Mehmet Alpaslan Köroglu. Flexural behavior of hybrid FRP/steel reinforced concrete beams. Composite Structures 129 (2015) 111–121.

51) Dipti Ranjan Sahoo, Kaushik Maran and Avdhesh Kumar. Effect of steel and synthetic fibers on shear strength of RC beams without shear stirrups. Construction and Building Materials 83 (2015) 150–158.

52) Biswarup Saikia, Phanindra Kumar, Job Thomas, K.S. Nanjunda Rao and Ananth Ramaswamy. Strength and serviceability performance of beams reinforced with GFRP bars in flexure. Construction and Building Materials 21 (2007) 1709–1719.

53) M. Pecce, G. Manfredi, and E. Cosenza. EXPERIMENTAL RESPONSE AND CODE MODELS OF GFRP RC BEAMS IN BENDING. JOURNAL OF COMPOSITES FOR CONSTRUCTION, 2000, 4(4): 182-190.

54) Habeeb M. N. Ashour A. F. (2008). Flexural Behavior of Continuous GFRP Reinforced Concrete Beams.

55) Maher A. Adam, Mohamed Said, Ahmed A. Mahmoud and Ali S. Shanour. Analytical and experimental flexural behavior of concrete beams reinforced with

glass fiber reinforced polymers bars. Construction and Building Materials 84 (2015) 354–366.

56) El-Mogy, M., El-Ragaby, A., and El-Salakawy, E. (2010). Flexural Behavior of Continuous FRP-Reinforced Concrete Beams.

57) Hannibal Ólafsson and Eyþór Þórhallsson. Basalt fiber bar Reinforcement of concrete structures. 2009.

58) M.E.M. Mahroug, A.F. Ashour and D. Lam. Experimental response and code modelling of continuous concrete slabs reinforced with BFRP bars. Composite Structures 107 (2014) 664–674.

59) A. Lapko and M. Urbański. Experimental and theoretical analysis of deflections of concrete beams reinforced with basalt rebar. Archives of civil and mechanical engineering 15 (2015) 223 – 230.

60) F. Ashour and M. N. Habeeb. CONTINUOUS CONCRETE BEAMS REINFORCED WITH CFRP BARS. 2008.

61) Pouya Banibayat and Anil Patnaik. Creep Rupture Performance of Basalt Fiber-Reinforced Polymer Bars. J. Aerosp. Eng. 2015.28.

62) Barris C. Torres Ll, Turon A, Baena M, Catalan A. (2009). An experimental study of the flexural behavior of GFRP RC beams and comparison with prediction models.

63) Kara, I. F., Ashour, A. F., & Dundar, C. (2013). Deflection of concrete structures reinforced with FRP bars. Composites Part B: Engineering, 44(1), 375-384.

64) Ju, M., Oh, H., Lim, J., & Sim, J. (2016). A Modified Model for Deflection Calculation of Reinforced Concrete Beam with Deformed GFRP Rebar. International Journal of Polymer Science, 2016.

65) ReforceTech, AS, www.ReforceTech.com, visited 25/04/2015.

66) Magmatech, www.magmatech.co.uk, visited 01/05/2016.

67) MateenBar, www.mateenbar.com, visited 01/05/2016.

68) ASTM D7205/D7205M-06, Standard Test Method for Tensile Properties of Fiber Reinforced Polymer Matrix Composite Bars, ASTM International, West Conshohocken, PA, USA, 2011.

69) ASTM C78-02, Standard Test Method for Flexural Strength of Concrete (Using Simple Beam with Third-Point Loading), ASTM International, West Conshohocken, PA, USA, 2002.

70) Kiang-Hwee Tan, P. Paramasivam, and Kan-Chai Tan. Creep and Shrinkage Deflections of RC Beams with Steel Fibers. J. Mater. Civ. Eng., 1994, 6(4): 474-494.

71) Teck-Yong Lim, P. Paramasivam, and Sing-Lip Lee, Fellow ASCE. Behavior of Reinforced Steel-Fiber-Concrete Beams in Flexure. J. Struct. Eng., 1987, 113(12): 2439-2458.

72) Lee and H. Kim. Orientation factor and number of fibers at failure plane in ring-type steel fiber reinforced concrete. Cement and Concrete Research 40 (2010) 810–819.

73) J.R. Yost, P. Gross, D.W. Dinehart, Effective moment of inertia for glass fiber reinforced polymer reinforced concrete beams, ACI Structural Journal 100 (6) (2003) 732–739.

74) S.S. Faza, H.V.S. GangaRao, Pre and post cracking deflection behavior of concrete beams reinforced with fiber reinforced plastic rebar, in: Proc., Advanced Composites Materials in Bridges and Structures, Canadian Society for Civil Engineering, Sherbrook, Que., Canada, 1992, pp. 151–160.

75) P.H. Bischoff, Deflection calculation of FRP reinforced concrete beams based on modifications to the existing Branson equation, Journal of Composites for Construction 11 (1) (2007) 4–14., http://dx.doi.org/10.1061/(ASCE)1090-0268 (2007)11:1(4).

76) P.H. Bischoff, S.P. Gross, Design approach for calculating deflection of FRP reinforced concrete, Journal of Composites for Construction 15 (4) (2011) 490–499. , http://dx.doi.org/ 10.1061/(ASCE)CC.1943-5614.0000195.

77) ISIS Canada, Reinforcing Concrete Structures with Fiber Reinforced Polymers. Design Manual N8 3 Version 2, Canada ISIS Canada Corporation, Manitoba, 2007.

78) CSA, S806-02: Design and Construction of Building Components with Fiber-Reinforced Polymers, Canadian Standards Association, Canada, 2007.

79) CEN 2004, Eurocode 2: Design of Concrete Structures – Part 1-1: General Rules and Rules for Buildings. PN EN 1992-1-1, European Committee for Standardization, Brussels, 2004.